

ISTANBUL TECHNICAL UNIVERSITY ★ GRADUATE SCHOOL OF SCIENCE
ENGINEERING AND TECHNOLOGY

DIESEL ENGINE EMISSIONS MODELING

M.Sc. THESIS

Yiğit KOYUNCUOĞLU

Department of Mechatronics Engineering

Mechatronics Engineering Programme

JANUARY 2013

ISTANBUL TECHNICAL UNIVERSITY ★ GRADUATE SCHOOL OF SCIENCE
ENGINEERING AND TECHNOLOGY

DIESEL ENGINE EMISSIONS MODELING

M.Sc. THESIS

Yiğit KOYUNCUOĞLU
(518101040)

Department of Mechatronics Engineering

Mechatronics Engineering Programme

Thesis Advisor: Prof. Dr. Metin GÖKAŞAN

JANUARY 2013

İSTANBUL TEKNİK ÜNİVERSİTESİ ★ FEN BİLİMLERİ ENSTİTÜSÜ

DİZEL MOTOR EMİSYON MODELLEMESİ

YÜKSEK LİSANS TEZİ

**Yiğit KOYUNCUOĞLU
(518101040)**

Mekatronik Mühendisliği Anabilim Dalı

Mekatronik Mühendisliği Programı

Tez Danışmanı: Prof. Dr. Metin GÖKAŞAN

OCAK 2013

Yiğit Koyuncuoğlu, a M.Sc student of ITU **Institute of / Graduate School of Science Engineering and Technology** student ID **518101040**, successfully defended the **thesis/dissertation** entitled “**DIESEL ENGINE EMISSIONS MODELING**”, which he prepared after fulfilling the requirements specified in the associated legislations, before the jury whose signatures are below.

Thesis Advisor : **Prof. Dr. Metin GÖKAŞAN**
Istanbul Technical University

Jury Members : **Assist. Prof. Dr Ali Fuat ERGENÇ**
Istanbul Technical University

Assist. Prof. Dr Pınar BOYRAZ
Istanbul Technical University

Date of Submission : 17 December 2012
Date of Defense : 25 January 2013

To Naime, Mehmet, Özge, Melih and Defne

FOREWORD

I heartily thankful to my advisor, Prof.Dr.Metin Göktaşan and his PhD student Mr. Bülent Ünver due to their great guidance in my thesis. A special thanks to my friends Çetin Gürel and Didem Aydın because of their assistance for dynamometer test data. I would also like to thank my girl friend Özge Ateş for her emotional support. Finally, I am very grateful to my family and my friends for their consideration and motivation.

January 2013

Yiğit KOYUNCUOĞLU
(Mechanical Engineer)

TABLE OF CONTENTS

	<u>Page</u>
FOREWORD	ix
TABLE OF CONTENTS	xi
ABBREVIATIONS	xiii
LIST OF TABLES	xv
LIST OF FIGURES	xvii
SUMMARY	xix
ÖZET	xxi
1. INTRODUCTION	1
1.1 Purpose of Thesis	2
1.2 Literature Review	2
2. EXPERIMENTAL SETUP	9
3. MODELLING METHODOLOGY	13
3.1 Genetic Algorithm Based Modeling Approach	13
3.1.1 Symbolic regression and GPTIPS toolbox	13
3.1.2 Derived model structures and their equations	15
3.1.3 Cylinder pressure based mass burned fraction modeling	18
3.2 Polynomial Based Regression Approach	25
4. RESULTS AND DISCUSSION	27
4.1 Results of Symbolic Regression Approach With Base Map	27
4.2 Results of Symbolic Regression Approach Without Base Map	32
4.3 Results of Polynomial Regression Approach	35
5. CONCLUSION	45
REFERENCES	49
CURRICULUM VITAE	53

ABBREVIATIONS

CFD	: Computational fluid dynamics
CHEMKIN	: Chemical Kinetics
CO	: Carbon monoxide
CTC	: Time Combustion Model
DOC	: diesel oxidation catalyst
DPF	: Diesel particulate filter
ECU	: Engine Control Unit
EGR	: Engine Control Unit
EOC	: End Of Combustion
GPTIPS	: Genetic Programming Toolbox
HC	: Hydrocarbon
HIL	: Hardware In the Loop
NO	: Nitric Oxide
NO_x	: Nitrogen Oxides
PM	: Particulate Matter
RMSE	: Root Mean Squared Error
SCR	: Selective Catalytic Reduction
SOC	: Start Of Combustion
SOI	: Start Of Injection
SR	: Symbolic Regression
WHTC	: World Harmonic Transient Cycle

LIST OF TABLES

	<u>Page</u>
Table 2.1 : Light duty diesel engine features	9
Table 2.2 : Measured channels from ECU and dynamometer	9
Table 3.1 : Symbolic regression parameters.....	14
Table 3.2 : Coefficients of the base map calculations for NO _x and PM.....	16
Table 3.3 : Model input channels	16
Table 3.4 : Coefficients of the equations from (3.2) to (3.7)	18
Table 4.1 : Overall Results	27

LIST OF FIGURES

	<u>Page</u>
Figure 1.1 : European emission standards for diesel engine passenger cars [3].	1
Figure 1.2 : Measured and estimated emission models with empirical model [5].	3
Figure 1.3 : The reduced input results with increased polynomial degree [5].	3
Figure 1.4 : Model Comparisons with measured data [6].	4
Figure 1.5 : Model validation results with transient test [9].	5
Figure 1.6 : CFD Grid of the one part of the cylinder [17].	6
Figure 1.7 : Calculated temperature and NO distribution inside the cylinder [17].	7
Figure 2.1 : Transient validation data and steady state modelling data.	10
Figure 2.2 : Pressure recordings taken from AVL IndiCom.	11
Figure 3.1 : Tree representation of symbolic regression [22].	14
Figure 3.2 : Model structure of the symbolic regression.	15
Figure 3.3 : Reduced model structure for symbolic regression.	17
Figure 3.4 : Mass burned fraction variations in gasoline engines [20].	19
Figure 3.5 : Normalized cylinder pressure at 2200 rpm and 131 N.m load.	20
Figure 3.6 : Illustration of EOC from the derivative of cylinder pressure.	21
Figure 3.7 : Apparent heat release rate and cylinder pressure profile [26].	22
Figure 3.8 : Comparison of methods given in equations (3.9) and (3.11).	22
Figure 3.9 : Modeled mass burned fraction with Wiebe approximation.	23
Figure 3.10 : Cylinder pressure based burned mass fraction curves.	24
Figure 3.11 : 'm' coefficients that best fitting the Wiebe function to the (3.11).	24
Figure 3.12 : 'a' coefficients that best fitting the Wiebe function to the (3.11).	25
Figure 3.13 : Model structure of polynomial regression.	26
Figure 3.14 : Flow chart of the polynomial based regression approach.	26
Figure 4.1 : Base map distribution of NO _x used in symbolic regression.	28
Figure 4.2 : Base map distribution of PM used in symbolic regression.	28
Figure 4.3 : Normalized NO _x simulation results with %50 MBF as 9th input.	29
Figure 4.4 : R square results of NO _x with %50 MBF as 9th input.	29
Figure 4.5 : Normalized NO _x results with start of main injection as 9th input.	30
Figure 4.6 : R square results of NO _x with start of main injection as 9th input.	30
Figure 4.7 : R square results of PM with %50 MBF as 9th input.	31
Figure 4.8 : Normalized PM simulation results with %50 MBF as 9th input.	31
Figure 4.9 : Normalized PM results with start of main injection as 9th input.	32
Figure 4.10 : R square results of PM with start of main injection as 9th input.	32
Figure 4.11 : Normalized NO _x results with start of main injection as 8th input.	33
Figure 4.12 : R square results of NO _x with start of main injection as 8th input.	33
Figure 4.13 : Normalized PM simulations with start of main injection as 8th input.	34
Figure 4.14 : R square results of PM with start of main injection as 8th input.	34
Figure 4.15 : Steady state NO _x results.	35
Figure 4.16 : Steady state NO _x R square results.	36
Figure 4.17 : Steady state PM results.	37

Figure 4.18 : R square results of steady state PM estimation.	37
Figure 4.19 : WHTC results of the NOx.	38
Figure 4.20 : WHTC R square results of the NOx.	39
Figure 4.21 : WHTC tracing of the simulated NOx.	40
Figure 4.22 : NOx results with mean value engine model [27].	41
Figure 4.23 : R square results of the NOx with mean value engine model [27].	41
Figure 4.24 : WHTC results with different calibration.	42
Figure 4.25 : R square results of second calibration validation.	42
Figure 4.26 : Effets of calibration change on NOx values.	43

DIESEL ENGINE EMISSIONS MODELING

SUMMARY

In this thesis, a heavy duty diesel engine emissions model is developed. The aim of the modeling is constructing a model structure that could be used for diesel engine calibration and control algorithm development.

The main constraints for modeling are that the inputs of the model could be feed from a mean value engine model. This means that the created model could easily used in HIL simulations. For modeling approach, data is gathered from the dynamometer located in Ford-Otosan test center. Because of company privacy policy, results and data are given as normalized form.

There are 2 types of data collected from the test bed. The first one is the modeling data which is recorded as steady state. While collecting data, the dynamometer run on the pedal-speed mode. Pedal changes from 0 to 100 percent and speed changes from 800 to 4500 rpm. For each pedal-speed point , reference maps of the ECU had changed. By this way, we expected high accuracy in our simulations for even if the calibration changes. The second the data is collected as transient. The test cycle is the world harmonized transient cycle. This data is used as the validation data.

The model inputs are, engine speed, injection timings, injection quantities, intake manifold pressure, intake mass air flow and rail pressure. Because the quantities of the nitrogen oxides and particulate matters constitute the biggest portion of the emissions, they are chosen as the output of the model.

During the literature survey, it is seen that the combustion center is chosen as input for the modeling. Therefore, with the scope of this thesis, combustion center is modeled with the help of measured cylinder pressure curves for each operating point.

There are 2 types of analysis applied. The first one is the genetic algorithm based regression modeling. With this method, model structure is created according to symbolic regression fundamentals. As a result of symbolic regression approach, it is observed that, the generated regression models are highly nonlinear and not reproducible. This means that, the model is highly sensitive to correlations between the inputs. The second method is the polynomial based regression approach. For this method, a polynomial equation is created. Then, best fitted coefficients are found by using modeling data. The created model is validated by using 2 recordings of the WHTC, which are recorded with different calibration.

Acceptable accuracy in NO_x and PM has been achieved for both modeling and validation data. As a result, the generated model takes its inputs from a mean value engine model easily. Then, the model could be used for diesel engine calibration process and control algorithm development in te HIL environment.

DİZEL MOTORU EMİSYON MODELLEMESİ

ÖZET

Günümüz de artan hava kirliliği sebebiyle atık gazların salınımına devletler tarafından limitler getirilmektedir. Hava kirliliği insan sağlığına zarar verdiği gibi dünyamıza da zarar vermektedir. Artan karbondioksit seviyeleri sera gazı etkisi yaparak dünya atmosferinin gereğinden fazla ısınarak iklimlerin değişmesine sebep olmakta ve ekolojik dengeyi bozarak bir çok canlının yok olmasına neden olmaktadır.

Dizel motorlardaki başlıca havayı kirleten egzoz gazları partikül madde (PM), azotoksitler (NO_x), hidrokarbon (HC) ve karbonmonoksittir (CO). Azotoksitler atmosfer de nitrik asit olarak birikerek asit yağmurlarına sebep olmaktadır. Partikül madde ise ekolojik etkiler ve görünürlük gibi çevresel etkileri bilinmektedir. Ayrıca partikül maddenin bronşit, akciğer kanseri ve astım gibi hastalıklara sebep olduğu bilinmektedir.

Dizel motor üreticilerinin emisyonları azaltmak için başlıca uygulamaları; motor tasarımında iyileştirmeler, yüksek basınçlı yakıt püskürtme sistemlerinin kullanılması, aşırı doldurma sistemlerinin tasarıma dahil edilmesi, egzoz gazının tekrar yanma odasına beslenmesi, yakıt formülündeki iyileştirmeler, yanma sonrası emisyon azaltıcı sistemlerin kullanılması şeklinde özetlenebilir. Sadece motor kalibrasyonunun en optimum emisyonu vericek şekilde yapılması ile istenen emisyon seviyelerine ulaşılamamaktadır. Bunun sebebi partikül madde ile azot oksitlerinin oluşumu arasındaki ters orantıdır. Dizel motorlarda azot oksitler, yanma alev sıcaklığının 1800 K olduğu kısımlarda oluşur. Partikül madde ise ısının düşük olduğu bölgelerde meydana gelir. Yanma odasının sıcaklığının düşürülmesi partikül madde oluşumunu artırırken azot oksit oluşumunu azaltacaktır. Ters durumda ise yanma odası sıcaklığını partikül maddeyi azaltacak oranda artırırsak bu sefer de azot oksit oluşumu için elverişli bir ortam oluşacaktır.. Bu durum, egzoz limitlerine uygun araçlar üretilmesi için yanma sonrası cihazların geliştirilmesini gerekli kılmıştır. Bilinen en önemli partikül azaltıcı yanma sonrası cihazı, dizel partikül filtresi (DPF) 'dir. Dizel partikül filtresi egzoz yolu üzerine monte edilerek egzoz gazı içerisindeki partikülleri hapseder. Bu durum bir süre sonra filtrenin dolmasına sebep olur. Filtrenin dolup dolmadığı ise, filtrenin giriş ve çıkış basıncını gözlemleyen bir sensör aracılığı ile motor kontrol ünitesi (ECU)' ne iletilir. Motor kontrol ünitesi gerekli eyleycilerini kullanarak egzoz hava sıcaklığını artırır. DPF ' te biriken partikül maddeyi yakar. Bu sayede temizlenen filtre ile motor normal çalışma moduna geri döner.

Araçlarda kullanılan bir diğer yanma sonrası cihazı ise seçici katalitik indirgeme (SCR) cihazıdır. SCR azot oksitlerin indirgenmesini oksitleyici bir atmosfer yaratarak sağlar. Sistemin seçici olarak adlandırılmasının sebebi NO 'in amonyak ile (NH_3) katalitik olarak indirgenmesinde oksijenin amonyakla oksidasyonuna tercihi olarak meydana gelmesindendir. SCR'nin bir kaç tipi vardır. Hangi katalistin

seçileceğini sistemdeki egzoz gazı sıcaklığı belirler. SCR'nin performansı katalistin sıcaklığına çok bağlıdır. Amonyak egzoz gazında üretmek için en iyi kaynak sulu üre çözeltisidir. Üre çözeltisi %32.5 üre ve %67.5 su içerir. Bu çözelti, SCR'den önce özel enjektörler aracılığı ile egzoz gazına püskürtülür. Püskürtülen üre su karışımı bozunarak amonyağı oluşturur. Amonyak SCR içerisindeki katalizörün yüzeyine yapışır. Yüzeydeki tepkimeye NO, NO₂ girer ve çıkış olarak daha az zararlı CO₂, H₂O ve N₂ oluşur. Bu sayede NO_x indirgenmiş olur. Sulu üre çözeltisinin püskürtme miktarı çok iyi kontrol edilmesi gereki. Aksi takdirde az püskürtülen çözelti NO_x salınımını artırırken, fazla püskürtülen çözelti istenmeyen NH₃'ün egzoz dan atılmasına sebep olur. SCR sistemleri 500 ile 900 K gibi bir sıcaklık aralığında çalışır. Sistemin en büyük dezavantajı hasas bir kontrol tekniğinin geliştirilmesini gerektirmesidir. Araçlar da SCR kullanımı WHTC gibi test çevrimlerin de NO_x emisyonlarını %80, HC emisyonlarını %90, partikül emisyonlarını ise yaklaşık % 40 azaltmaktadır.

Bu tez çalışmasında ağır yük dizel motoruna ait emisyon modeli geliştirilmiştir. Modellemede ki hedef, dizel motor kalibrasyonun da ve kontrol algoritması geliştirmede kullanılabilecek bir model yapısı geliştirmektir. Modellemede ki başlıca kısıt, model girişlerinin kontrol algoritması geliştirmek için oluşturulmuş basit bir dizel motor modelinden beslenebilmesi gereğidir. Bunun anlamı, oluşturulan modelin donanımla benzetim (HIL) simülasyonlarında dizel motor modeli ile beraber kolayca kullanılabilmesidir. Model yaklaşımı için, gerekli data Ford-Otosan test merkezindeki dinamometreden toplanmıştır. Şirket gizlilik ilkeleri sebebiyle, tezde kullanılan data ve sunulan sonuçlar normleştirildikten sonra teze eklenmiştir. Dinamometreden 2 tip data toplanmıştır. Bunlardan ilki modelleme de kullanılan durağan durum datasıdır. Data toplama işlemi yapılırken, dinamometre pedal-hız modunda çalıştırılmıştır. Pedal değerleri 0 ile 100 arasında değişirken, motor hızı değerleri 800 ile 4500 rpm arasında değiştirilmiştir. Herbir pedal-hız çalışma noktasında, elektronik kontrol ünitesindeki referans haritaları belli aralıklarda değiştirilerek data toplanmıştır. Bu sayede, bu datayı kullanarak yaptığımız modelin, kalibrasyon değişikliği yapılsada hassas sonuçlar vermesi beklenmiştir. Diğer data ise kısa süreli geçişler ile toplanmıştır ve uygulanan çevrimin bilinen ismi WHTC'dir. Bu data model doğrulama datası olarak kullanılmıştır.

Model girişleri, motor hızı, enjeksiyon zamanlamaları, enjeksiyon miktarları, manifold giriş basıncı, manifold hava debisi ve ortak ray basıncıdır. Modelleme de kullanılan girişler dinamometrede ekstra sensör ihtiyacı gerektirmemiştir. Bunun sebebi motora bağlı olan sensörlerin motor tasarımına ait sensörler olmasıdır. Bu sensörler için ekstra enstrümantasyon yapılmaması data toplamada ECU nun sensörlerden ölçtüğü bilginin direk kullanılabilmesini mümkün kılmıştır. Ancak PM ve NO_x sensörleri motorun standart yapısında bulunmamaktadır. Bu sebeple dinamometrede bu sensörler motor egzoz çıkışında, turbo makinadan biraz ileride monte edilmiştir.

NO_x sensörü ölçümlerini milyonda partikül(ppm) olarak yapmaktadır. Sensörün ölçüm aralığı 0 ile 1500 ppm'dir. NO_x sensörü yapısında 2 katman bulundurmaktadır. 1. katmanda havanın içindeki oksijeni iyonlarına ayıran oksitleyici elektrot vardır. Oksitlenme sonucu ortaya çıkan negatif yükler karşı elektrotta elektrik akımı başlamasına sebep olur. Sensöre gelen hava yoğunluğuna göre bu elektrik akımı değişiminden oksijen oranı ppm olarak saptanır. 2. katmanda ise NO_x miktarı saptanır. 2. katmanın hemen altında ki ısıtıcı sayesinde NO molekülleri O₂ ve N₂ moleküllerine ayrışır. 1. katmandaki prensip 2. katman da

mevcuttur ve NO molekülleri sebebiyle açığa çıkan O₂ miktarı bir önceki katmanda hesaplanan O₂ miktarından çıkartılarak NO kaynaklı oksijen miktarı bulunur. NO kaynaklı oksijen miktarının 2 katı kadarı egzoz gazı içerisindeki azot oksit miktarının ppm olarak algılanmasını sağlar.

PM ölçümü ise beyaz bir filtre yardımı ile sağlanmıştır. Partikül madde sensör içerisine alındıktan sonra filtre kağıdından geçirilmiştir. Filtre kağıdının hemen üzerinde bir ışık kaynağı vardır. Işık kaynağı ışınlarını filtre kağıdına gönderir. Filtre kağıdından yansıyan ışığın dalga boyu algılayıcı tarafından hissedilir. Filtre kağıdında biriken partikül madde daha fazla ışığın yansıtılmasını sağlar. Detektör de bu sayede partikül maddeden yansıyan ışığın dalga boyuna göre bir sinyal üretir. Partikül madde filtre islenme sayısı (FSN) olarak bilinen cinsten 0 ile 10 arasında ölçüm yapar. Filtre kağıdının hiç islenmemiş halindeki ve tam islenmiş halindeki ışığı yansıtması sonucu oluşan gerilimler bilinmektedir. Filtre kağıdının islenmesi sonucu oluşan ara sinyaller 0 ile 10 arası yapılan interpolasyon yardımıyla belirlenir.

Dizel motor emisyonları içinde, en yüksek emisyon miktarları, nitrojen oksitleri ve parçacıklı maddeye ait olduğu için, model çıkışları olarak bu iki değer hesaplanmıştır. Literatür araştırmasın da, yanma merkezi değerinin, yanma modeli girişi olarak kullanıldığı saptanmıştır. Bu sebeple, bu tez çalışması kapsamında, yanma merkezi kontrol amaçlı kullanılan dizel motor modeli çıkışı olmamasına karşın, silindir içi basınç değerleri yardımıyla modellenmeye çalışılmıştır. Elde edilen yanma merkezi değerleri modele giriş olarak beslenmiş ve model hassasiyetine olan etkisi gözlemlenmiştir. Tez çalışması kapsamında 2 farklı modelleme yaklaşımı uygulanmıştır. İlk metot, genetik algoritma tabanlı sembolik regresyon analizidir. Bu metodun uygulanması sonucunda, elde edilen model yapıları aşırı derece de doğrusal olmayan ve tekrar üretilemeyen denlemlerdir. Model yapısının aşırı derece de doğrusal olmayışı, modelin girişlerinin birbiri arasındaki ilişkisine çok hassas olmasına sebep olmaktadır. Tez çalışması kapsamında uygulanan bir diğer metod ise, polinom bazlı regresyon analizidir. Bu amaçla, polinom bazlı denklem yapısı belirlendikten sonra, modelleme datasını en hassas tutturan katsayılar bulunmuştur. Polinom bazlı model yapısı, farklı kalibrasyonlar ile koşturulmuş 2 WHTC testi ile doğrulanmıştır. Elde edilen sonucun NO_x ve PM için kabul edilebilir hata oranlarına sahip olduğu görülmüştür. Sonuç olarak model girişlerini kontrol amaçlı geliştirilmiş basit bir motor modelinden alabilen, kalibrasyon değişikliğine dayanıklı, kalibrasyon ve kontrol algoritması çalışmaların da ve HIL simülasyonların da kullanılabilecek bir emisyon modeli oluşturulmuştur.

1. INTRODUCTION

Diesel engines have important place in the transportation area because of their lower fuel consumption contrast to gasoline engines. They are widely used in the vessels, passenger cars, heavy duty trucks, light duty trucks, helicopters and unmanned air vehicles. The most known disadvantage of the diesel engine is its high emissions. Especially, nitrogen oxides (NO_x) and particulate matter (PM) [1]. Because these emissions are harmful for the environment and all leaving cratures in the world, challenging emissions legislations as denoted in Figure 1, forces motor companies to reduce the pollutant emissions of the diesel engines. For this purpose, diesel engines are equipped with many devices such as DPF, SCR, EGR, DOC and ECU. The DPF is intended to reduce PM emissions, while SCR, and EGR have been used to reduce the NO_x. Morower, to supply more fresh air turbochargers and superchargers have been added in to diesel engine structure while increasing its performance [2]. The most important device is the ECU which actuates all of the above equipments by the help of measurement sensors mounted on the engine . By controlling the injectors with ECU, different injection strategies are applied to improve the in cylinder pollutant formation.

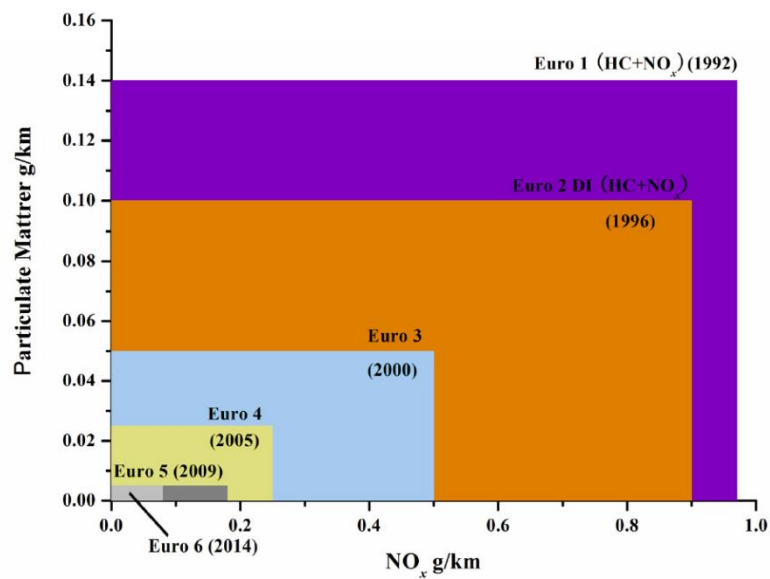


Figure 1.1 : European emission standards for diesel engine passenger cars [3].

1.1 Purpose of Thesis

The purpose of this thesis is to create a model of diesel engine emissions NO_x and PM. The model shall be used in the engine calibration process and control algorithm development. The model should have the below capabilities,

- Acceptable accuracy with the validation data which is recorded as transient.
- Model inputs shall be supplied from ECU or from a mean value diesel engine model.
- It shall be work faster than real time.
- It shall easily be conducted with the Hardware In the Loop (HIL) simulator models.
- Model should be capable of calculating the emissions accurately even if a calibration change occurs.
- Model should be applicable for any engine with a low tuning effort.

1.2 Literature Review

Predicting formation of the pollutant in diesel engine is not easy both numerically and theoretically. The complexity of modelling comes from the combustion phenomena. Combustion event is a time dependent function of air fuel mixture distribution, pressure and temperature of the in cylinder [4].

In the literature, mainly there are 3 types of modelling approaches which are:

- Empirical models
- Phenomenological models
- Models predicted by computational fluid dynamics (CFD)

An example empirical emissions model to predict the nitrogen oxides and particulate matter is present by the [5]. The author is aimed to create a mean value engine model for engine control algorithm development purposes. To support this engine model , he predicted the emissions NO_x and PM by using a polynomial function. The model inputs are fuel flow, engine speed, exhaust manifold temperature, start of injection,

air flow and air to fuel ratio. The maximum degree of the polynomial model is second order and the number of coefficients are 21.

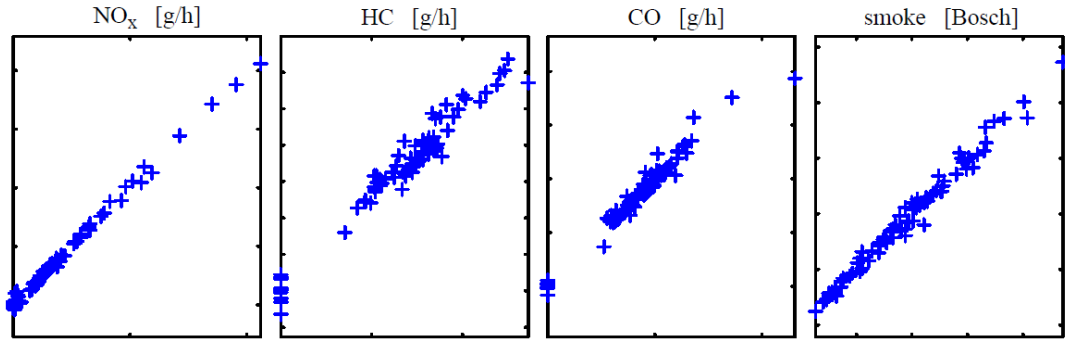


Figure 1.2 : Measured and estimated emission models with empirical model [5].

After getting these results, author has applied a simple analysis on the models. He tried to reduce inputs. To predict the NO_x, a third order polynomial is created with the model inputs, engine speed and fuel flow. For HC, CO and PM, engine speed, fuel flow and SOI is used as input up to third degree and the results are given in Figure 1.3.

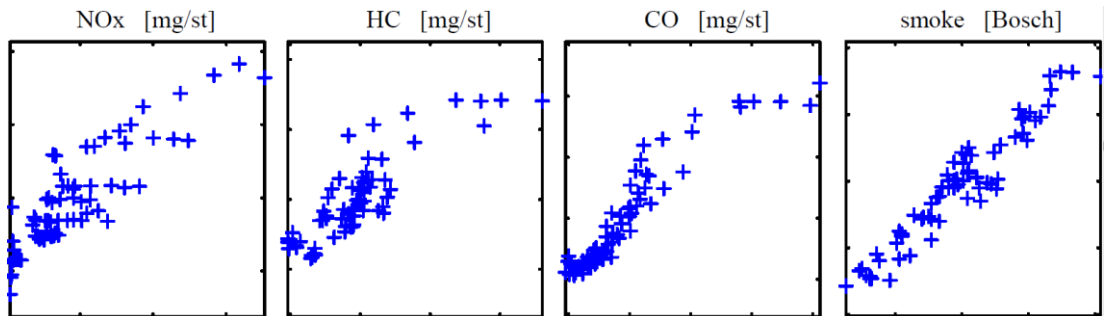


Figure 1.3 : The reduced input results with increased polynomial degree [5].

The emission estimation method is concluded with these analysis. The results show that increasing the degree of polynomial decreased the accuracy, and according to author, validation simulations predicts the emissions with the same performance contrast to second degree structure, but increasing coefficients yields becoming over-parametrizing and being sensitive to the inputs variations that results poor quality of the emissions estimation.

A phenomenological soot model has been introduced by the [6]. The author has used the most famous soot modelling approach conducted by Hiroyasu [7] [8]. Hiroyasu stated that the total soot mass generated by the 1 cycle of the internal combustion engine is the difference between soot formation and soot oxidation.

$$m_s = m_F - m_O \quad (1.1)$$

Hiroyasu has created a model structure to reach an acceptable accuracy with his empirical experiences.

The A_F and A_O are just the calibration parameters of the equations which are tuned with the soot measurement data. The activation and formation energies are denoted by E_F and E_O . According to the author p is used as a correction term. The m_B is the rate of burned mass according to the crank angle φ . R is the gas constant and the T is incylinder temperature. If we looked again the equations (1.2) and (1.3), formation rate depends on the burned mass rate while the oxidation rate depends to the soot itself.

$$\frac{dm_F}{d\varphi} = A_F \cdot \frac{dm_B}{d\varphi} \cdot p^{0.5} \cdot \exp\left(-\frac{E_F}{R.T}\right) \quad (1.2)$$

$$\frac{dm_O}{d\varphi} = A_O \cdot m_s \cdot O_2 \cdot p^{1.8} \exp\left(-\frac{E_O}{R.T}\right) \quad (1.3)$$

This means that more soot inside the cylinder increases the soot oxidation and that decreases the formation of the soot while the crank angle increases.

Figure 1.4, gives the estimated tailpipe soot which is modeled with the Hiroyasu method and Hiroyasu based method JKU applied by the Joseph and Daniel [6].

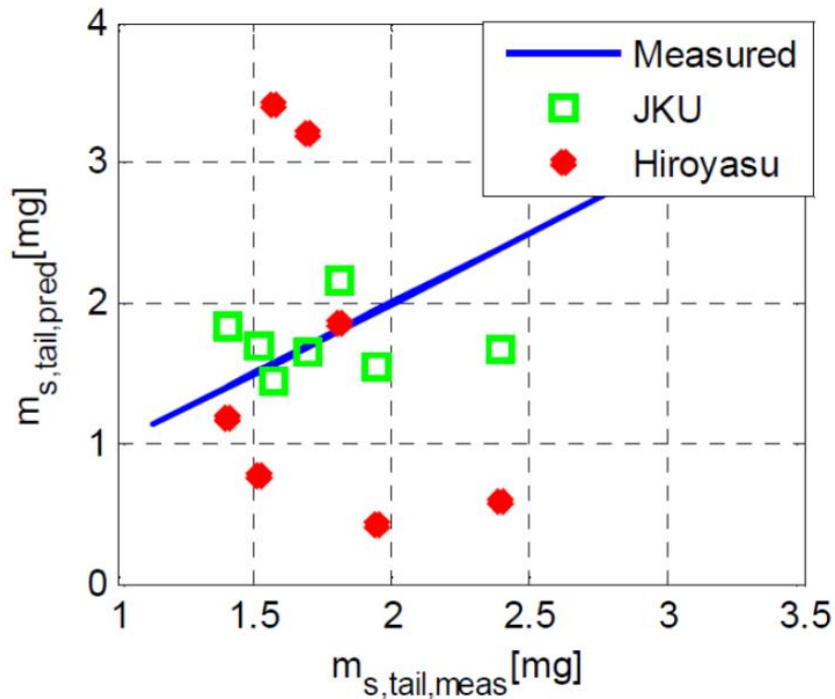
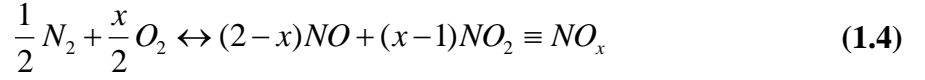


Figure 1.4 : Model Comparisons with measured data [6].

A phenomenological NO_x model has been released by the Professor Guzzella and his students [9]. The aim of the represented work is creating a novel NO_x modelling method with a high accuracy. The created model is aimed to use in control algorithm development. Basic structure of the model is the well known Zeldowich mechanism as explained in the [10, 11, 12].

He has formulated the equation (1.4) with the forward and backward reaction rates r_{fw} and r_{bw} as in the equation (1.5).



$$r_{fw} = k_{fw}(\mathcal{G}) \cdot [N_2]^{\frac{1}{2}} \cdot [O_2]^{\frac{x}{2}} \quad r_{bw} = k_{bw}(\mathcal{G}) \cdot [NO_x] \quad (1.5)$$

The \mathcal{G} corresponds to the in cylinder temperature of the diesel engine. In the (1.6), he conducted that the net reaction rate is the difference between the forward and backward reactions times the volume in which the reaction occurred. Finally, he get the total amount of NO_x formation with equation (1.6)

$$\frac{n_{NO_x}}{6.N_{eng}} = \int_{\varphi_{SOC}}^{\varphi_{EVO}} V_{reac}(\varphi) \cdot (r_{fw}(\varphi) - r_{bw}(\varphi)) d\varphi \quad (1.6)$$

The main point of this application while estimating the NO_x formation is the assumptions made and converting the above equations to a parametric form. After converting the parametrized form, a phenomenological equation structure is created for tuning purposes by using an appropriate cost function to get best fitted parameter set. The detailed formulations can be found in the [9].

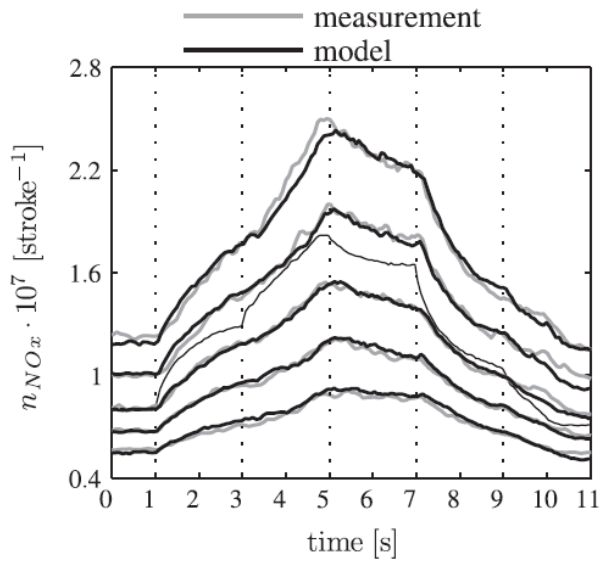


Figure 1.5 : Model validation results with transient test [9].

Validation results shows a good estimation of the measured transient data. According to the authors generated structure of the model requires low measurement points for tuning of the parameters and it is applicable to the different engines with a low modelling effort.

Finally, even if the CFD derived modelling approaches are not appropriate solutions for control algorithm development purposes, with the scope of literature survey of this thesis and having better understanding of the emissions modelling problems, it is valuable trying to understand the conducted solutions utilizing from the CFD.

There are many examples of CFD based combustion modelling as released in the following works [13,14,15]. The KIVA-3vr2 code usually is used as a CFD environment [16]. In CFD applications, all aspects of combustion process can be modeled with higher accuracy than the empirical and phenomenological models. Usually, the engineers and researchers tried to model in cylinder pressure, heat release rate of the cylinder and formed pollutant emissions NO_x and PM. There are 2 types of combustion modelling methods which are Characteristic Time Combustion Model (CTC) and more detailed combustion model CHEMKIN which mean is chemical kinetics [16]. In CFD applications, firstly a fuel spray grid is generated as given in Figure 6. Then the differential equations of the each models that can be CTC or CHEMKIN is solved for each nodes of the grid. The emissions amount, pressure and temperature are all solved for these nodes.

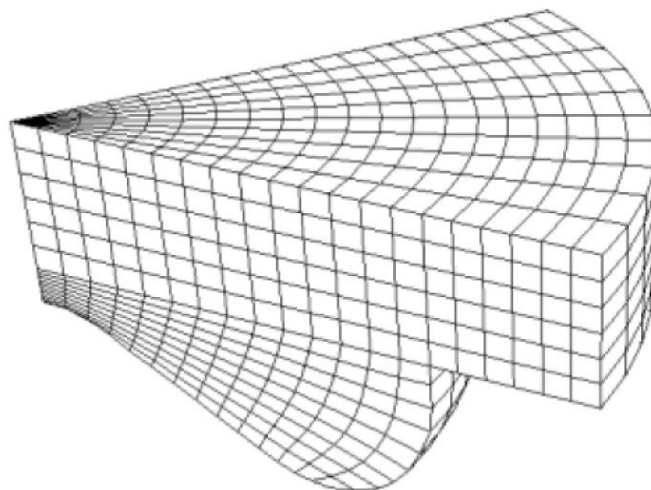


Figure 1.6 : CFD Grid of the one part of the cylinder [17].

If we looked into the Figure 1.7 NO and temperature distribution of the combustion chamber is modeled for different crank angles [17].

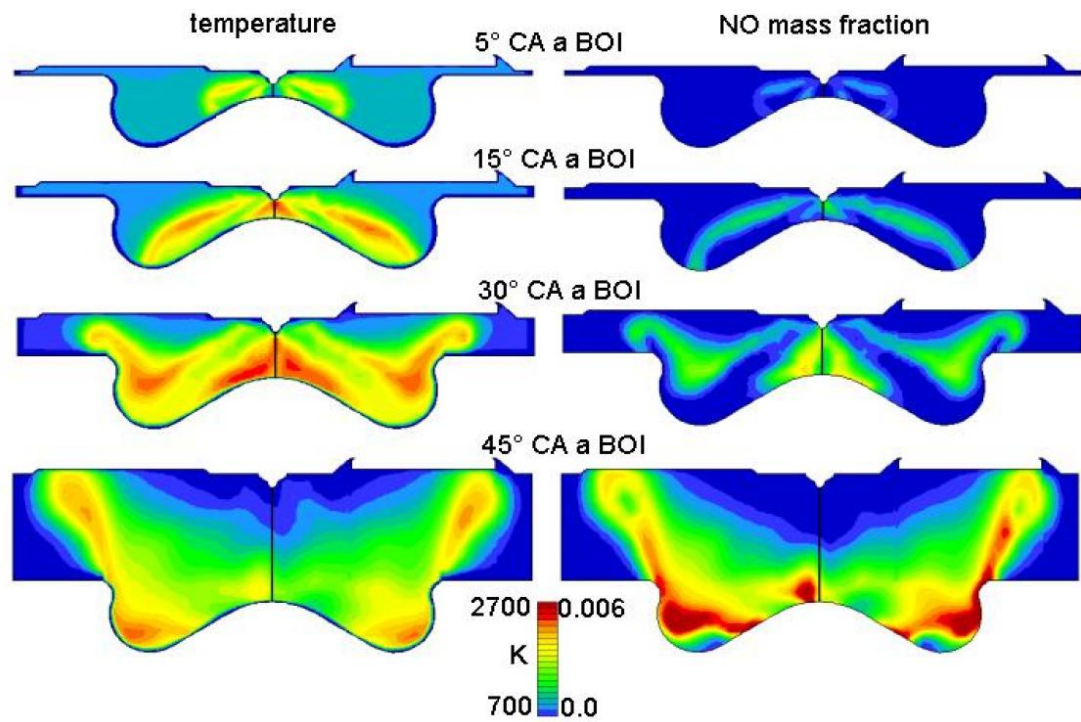


Figure 1.7 : Calculated temperature and NO distribution inside the cylinder [17].

As a result, for control algorithm development purposes, phenomenological and empirical modelling approaches are widely used in the literature.

2. EXPERIMENTAL SETUP

The measurements are gathered from a heavy duty diesel engine connected to the the Ford-Otosan dynamometer. Its main features are given in Table 2.1. It is a modern common-rail direct injection diesel engine mounted with an EGR Valve, EGR Cooler, VGT turbocharger. The diesel engine smoke measurements are collected with an AVL 415 S smoke meter at the outlet of the exhaust manifold. For measuring principles of smoke meter please see the reference [28]. Moreover, NO_x measurements are gathered from AVL AMA i60 exhaust measurement system and its measuring fundamentals are given in [29]. Furthermore, the in cylinder pressures are also recorded as crank angle resolved by using an AVL IndiCom system to estimate the in cylinder characteristics such as fuel burned mass fraction.

Table 2.1 : Heavy duty diesel engine features.

Engine Type	Heavy - Duty
Air path Equipments	Air Filter, EGR, VGT Turbo
Fuel Injection	Common Rail - DI
Number Of Cylinders	4

The measurements are recorded as steady state for each operating point on the AVL chassis dynamometer. Taking steady state measurements make easy to synchronize the measurements taken from ECU and dynamometer. logged measurement channels are given in Table 2.2. Engine speed and torque information are taken from directly dynamometer controller. The timings of main injection, pilot injection, and their quantities are swept around the speed and torque characterized operating points to better map the world harmonic transient cycle (WHTC).

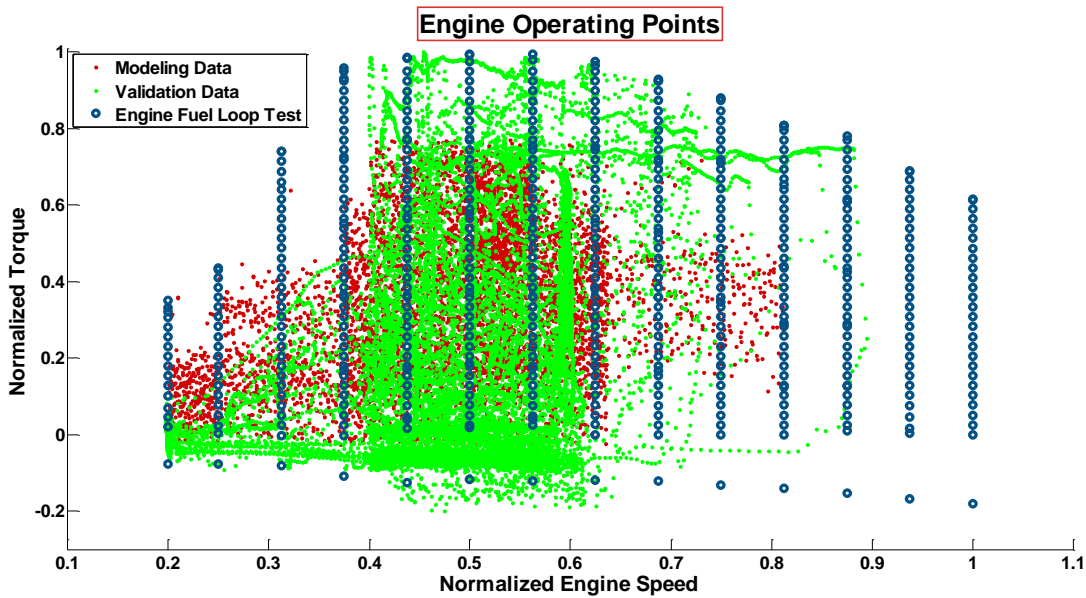
Table 2.2 : Measured channels from ECU and dynamometer.

Channel Name	Measurement Device	Range
In cylinder pressure (bar)	AVL IndiCom	1-190
NO _x , CO ₂ (ppm)	AVL AMA i60	10-2500
Soot (FSN)	AVL 415S	0.01-9
Boost pressure (mbar)	ECU	1000-2800
Air flow (mg/str)	ECU	250-1400
Start of Main Injection (CA)	ECU	-10-10

Table 2.2 : Measured channels from ECU and dynamometer (continued).

Start of Pilot Injection (CA)	ECU	-10-10
Main Injection Quantity (mg/str)	ECU	0.01-35
Pilot Injection Quantity (mg/str)	ECU	0.01-35
Manifold Temperature (C ^o)	ECU	23-270
Engine Speed (rpm)	Dyno Controller	800-3300

Figure 2.1 gives the validation and modelling data on the same plot. The WHTC cycle has 18003 recorded data points that are sampled with 0.1 seconds. Furthermore, emissions of the WHTC cycle is tried to model with 8000 points that are recorded as steady state aproximatly for each 60 seconds. The total time consumed for the testing is aproximatly 135 hours.

**Figure 2.1** : Transient validation data and steady state modelling data.

Due to the AVL S415 can not take transient recordings the generated PM model will be validated with steady state measurements. The NO_x records are captured transiently in WHTC, therefore the comparison of WHTC and modeled NO_x will be available for nitrogen oxides .

In the Figure 2.2 recorded pressure curves are given. These pressure curves are recorded as crange angle resolved and the resolution is 1 CA. In this thesis, these pressure curves are used to aproximate burned mass fraction. Normally, there is not any measuring method to collect burned mass fraction data. Usually, it is aproximated by using cyclinder pressure information as in the following works [19,

20, 21]. In this thesis, our aim is to develop a control oriented emissions model, therefore, in cylinder pressure is not an output of the mean value diesel engine model. %50 burned mass fraction is calculated by using the cylinder pressure and a second order polynomial model is fitted to the combustion center by using the measured channels .

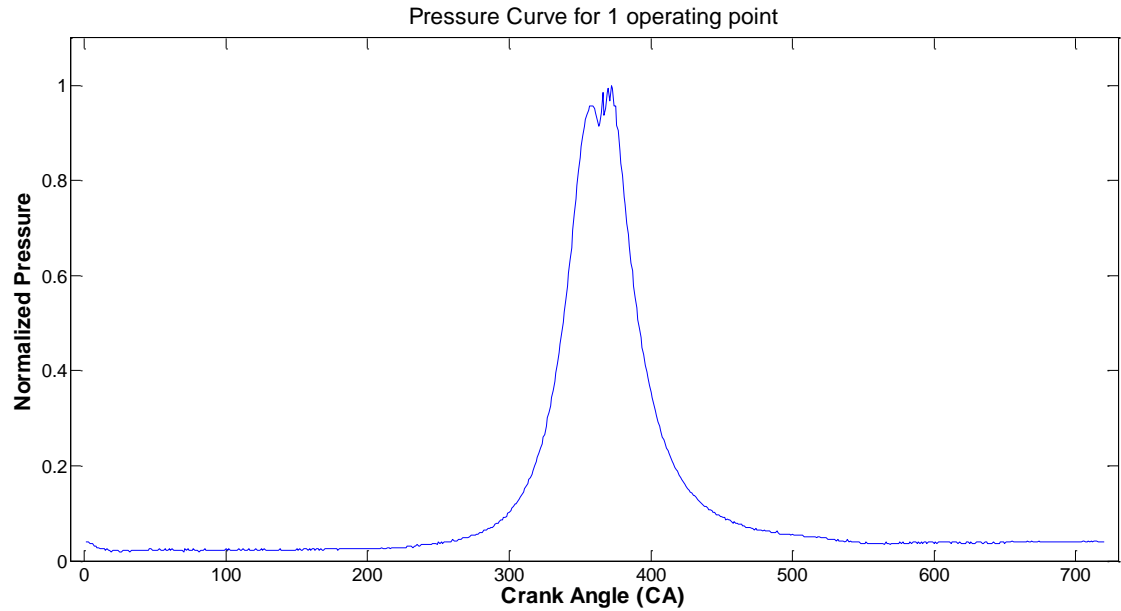


Figure 2.2 : Pressure recordings taken from AVL IndiCom.

3. MODELLING METHODOLOGY

The modelling methodology applied in this thesis is separated into two parts. The first method is inspired from the published doctoral dissertation [22]. The dissertation improved a novel method for control applications which is explained in the next section. The second method has a polynomial structure for modelling and a similar work is applied by the referenced work [5]. The inputs for both modelling applications are chosen according to empirical experiences and literature survey. It is seen that the most effective variables causing the formation of the NO_x and PM are rail pressure, manifold pressure, start of main and pilot injections, quantity of main and pilot injections, mass airflow of the intake manifold and the engine speed. In this thesis these variables and the values derived from these channels will be used as the inputs of derived models.

3.1 Genetic Algorithm Based Modeling Approach

In this method, the structure of the model is created by a symbolic regression algorithm (SR). For this purpose, a toolbox has been used which name is GPTIPS. This toolbox is developed by using the MATLAB programming environment. Some published papers for different areas are given in the official web site of the toolbox [23]. A simple check also carried out to test the reliability of the toolbox.

3.1.1 Symbolic regression and GPTIPS toolbox

Symbolic regression tries to find a function in symbolic form by using genetic programming fundamentals. The features of the symbolic regression are terminal set, function set and fitness evaluation [24]. It is useful to explain fundamentals of the symbolic regression used in the GPTIPS toolbox. Individuals called genes are represented by constants, functions and terminals. For example, "2 * X" is a single gen. In this gen, "2" is the constant term "X" is the terminal term and "*" is the function term. These gens which are generated randomly created the trees as in Figure 3.1.

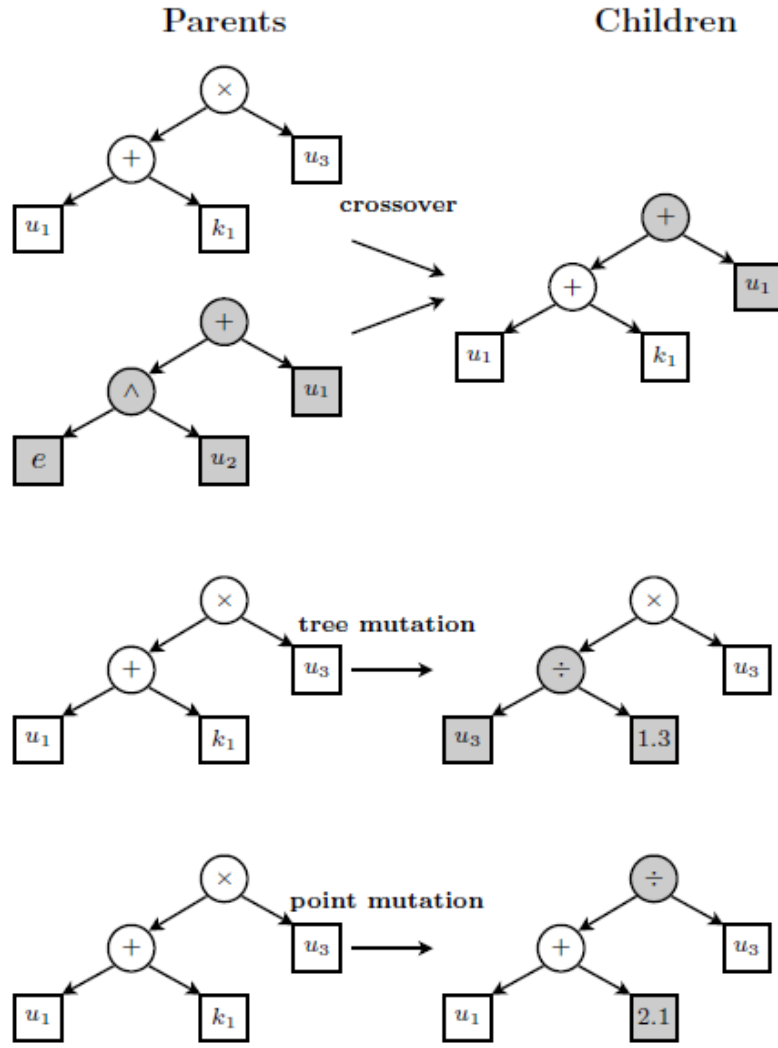


Figure 3.1 : Tree representation of symbolic regression [22].

Created tree is evaluated and if it does not meets the requirements of the fitness function it is manipulated by crossover, tree mutation and point mutation. GPTIPS works with a configuration script which is written in the MATLAB. The parameters of the symbolic regression algorithm is given in the Table 3.1.

Table 3.1 : Symbolic regression parameters

Parameter	Value
Population Size	100
Iteration Number	100
Fitness Function	RMSE
Maximum Gen Number	2
Functions	times-square-minus-divide
Mutation Rate	0.75
Crossover Rate	0.2
Maximum Tree Depth	5

3.1.2 Derived model structures and their equations

Mainly, there are 2 types of modelling approaches applied with symbolic regression. The first derived model has 2 parts. 1 part is base map of the relevant inputs and the second part is the generated symbolic equation. To better understand the structure let's see the Figure 3.2. The second derived model is directly generated with symbolic regression. Its block diagram representation is given in Figure 3.3.

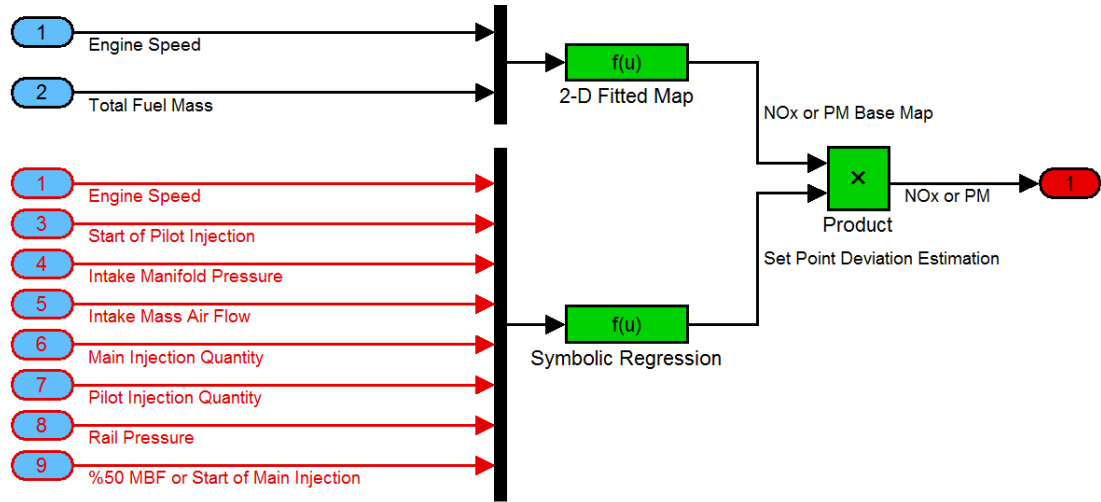


Figure 3.2 : Model structure of the symbolic regression.

As can be understood model has 9 inputs. The 9th input of the model is changed between the %50 mass burned fraction (%50 MBF and start of main injection. 4 different models are generated for NOx and soot. Because mass burned fraction values are not measured directly, their measured values are calculated by using the incylinder pressure values and explained in detail in the mass burned calculation section.

Engine speed and total injected fuel mass corresponds to the operating point of the diesel engine. The aim of creating a base map for NOx and PM is estimating the operating point values of the NOx and PM in steady state condition. During data collection, set point maps of the injection timing, injection quantities, manifold absolute pressure and mass airflow is swept from the ECU around the each operating points. Therefore we can call the symbolic regression output as set point deviation estimation.

To estimate the base values of the NOx and PM. A second order polynomial has been fitted. Please see below the structure of the used equation for PM and NOx base map estimation.

To find the values of the C1,C2,C3 and C4 NLINFIT function of the MATLAB is used. This function returns the best fitted coefficients of the given equation structure. In Table 3.2 estimated coefficients are given for NOx and PM respectively. C1, C2, C3 and C4 are the fitted coefficients. Moreover, X1 and X2 in (3.1) are the engine speed and total injected fuel mass into the cylinder.

$$C1 + C2 * X1 + C3 * X2 + C4 * X1 * X2 \quad (3.1)$$

Table 3.2 : Coefficients of the base map calculations for NOx and PM.

Model	C1	C2	C3	C4
NOx	243.0750	33.4172	0.1713	-0.0117
PM	0.8501	0.0125	-0.0002	0

2 Different model structures are generated with symbolic regression approach for PM and NOx estimation. The difference between the models is the 9th input. For the 1st case %50 MBF is used as the 9th input and for the second case start of main injection is used.

Derived model structures for NOx and PM are given below that uses %50 MBF as 9th input channel.

The model input names are given in the Table 3.3.

Table 3.3 : Model input channels.

Indices	Names
X1	Engine speed
X2	Start of pilot injection
X3	Intake manifold pressure
X4	Intake air mass flow
X5	Main injection quantity
X6	Pilot injection quantity
X7	Rail pressure
X8	Combustion center or Start of main injection

The model structures are ;

$$NO_x = \frac{c_1 x_2 x_4 x_8 (c_2 x_1 - c_3 x_5)}{x_1 (x_3 - x_4 + x_6 - x_7)} - \frac{c_4 x_4 (x_3 - x_8) (\frac{x_5 - x_7}{x_3 - x_4} + \frac{x_6}{x_7} - c_6)}{x_3 (x_3 - x_7)} - c_5 \quad (3.2)$$

$$PM = \frac{c_1 x_3 x_5 x_8 (x_3 x_8 - x_4^2)}{x_4^4 (x_2 - x_4)} + \frac{c_2 x_7 x_8 (x_2 - x_8)}{x_1 x_4 (x_1 - c_3) (x_5 - x_1 + x_6)} - c_4 \quad (3.3)$$

Because the mass burned fraction value is a start of main injection derived value. To see the effect of mass burned fraction, it is replaced by start of main injection value. Next equations are derived from the symbolic regression by using start of main injection instead mass burned fraction.

$$NO_x = c_1 x_2 (x_7 - x_8) - c_2 x_6 (x_1 x_5 - x_4^2) + \frac{c_3 x_4 x_7 (x_4 - x_7) (x_2 - x_3 + c_4)}{x_3 (x_3 - x_1)} - c_5 \quad (3.4)$$

$$PM = \frac{c_1 (x_3 + x_1 x_5 + x_3 x_5 - \frac{x_1}{x_6} - c_2)}{(x_2 - x_4)^2 - x_1 x_2 x_6} + \frac{c_3 x_3 (x_5 - c_4) (x_1 - x_4)}{x_7 (x_2 - x_4) (x_1 - x_8)} - c_5 \quad (3.5)$$

As a second method, to understand the disadvantages and advantages of a base map, it is removed from the model structure and the results are discussed in the results section.

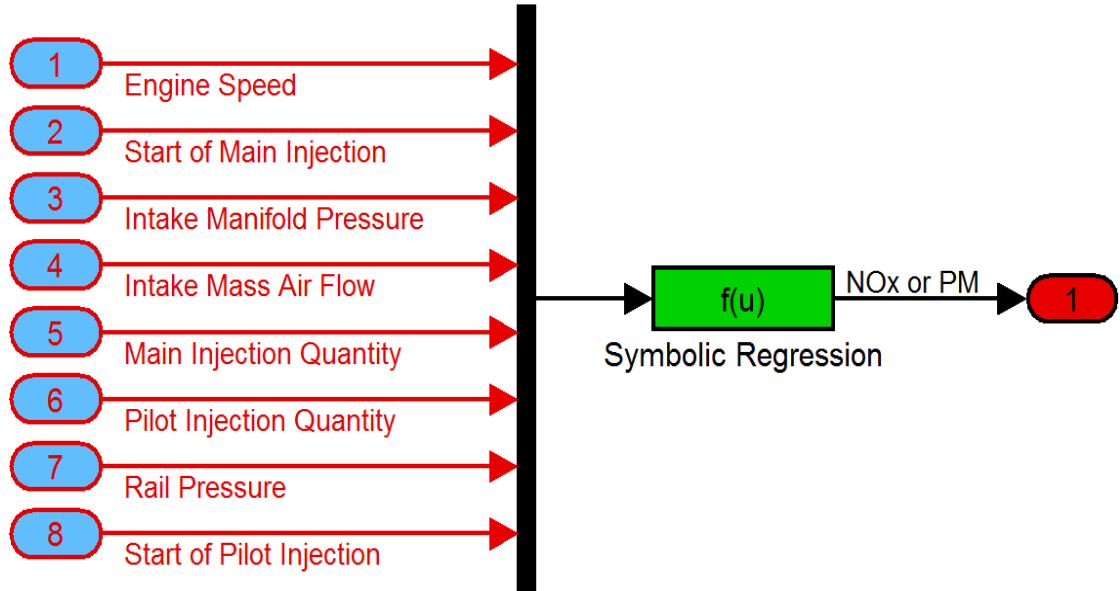


Figure 3.3 : Reduced model structure for symbolic regression.

Because using start of main injection or mass burned fraction has closer results, only the start of main injection has used as 8th input. The created model structures are given in (3.6) and (3.7) for NO_x and PM.

$$NO_x = \frac{c_1 (x_4 - c_2 x_7 + x_8 - \frac{x_3}{x_5})}{x_3 + \frac{c_3}{x_5} + \frac{x_1 x_3}{x_7}} + \frac{c_4 (x_2 - x_6) (x_7 - x_8) (x_4 - x_7 + \frac{c_5}{x_5})}{(x_2 - x_4)^2 - (x_3 - c_6) (x_1 - x_2)} - c_7 \quad (3.6)$$

$$PM = \frac{c_1 x_3 x_5}{(x_4 - x_5)^2} + \frac{c_2 x_5 (x_2 - x_3)}{x_4 (x_4 - x_5)} - \frac{c_3 (x_1 - x_5 x_7) (x_3 - x_7)}{(x_4 - x_5) (c_4 x_5 - c_5 x_7 + x_1 x_8 - c_6)} - c_7 \quad (3.7)$$

Please find the coefficients of equations 3.2 to 3.7 in Table 3.3.

Table 3.4 : Coefficients of the equations from (3.2) to (3.7).

Coefficients	3.2	3.3	3.4	3.5	3.6	3.7
C1	$1,991.10^{-7}$	752	0.0005214	11.39	40566	581.5
C2	8184	$4,596.10^7$	$1,036.10^{-7}$	-3673	2	581.5
C3	6908	3787	$5.536.10^{-7}$	0.01943	8907	57.37
C4	4818	0.005661	4942	2555	3139	1774
C5	-1.543	-	0.1781	1.334	7993	3923
C6	1	-	-	-	9088	12299
C7	-	-	-	-	106.2	-0.3999

3.1.3 Cylinder pressure based mass burned fraction modeling

From the literature survey, it is claimed that the mass burned fraction is highly effected on the resultant emissions [18, 22]. In this thesis, mass burned fractions are modeled as virtual sensor infomation and used in the symbolic regression calculations. Same effetcs on the emissions is aimed to be osberved.

Infact, the mass fraction burned is defined as ratio of heat release to the total heat release as shown in equation (3.8)

$$MFB(\varphi) = \frac{\int_0^{\varphi} \frac{dQ}{d\varphi}}{Q} \quad (3.8)$$

As can be seen from the equation (3.8) it is not easy to use this formulation with a control oriented mean value diesel engine model. Therefore, usually this equation is estimated with Wiebe function. A simplified formulation of the Wiebe function is given in equation (3.9)

$$MFB(\varphi) = 1 - \exp\left[-a\left(\frac{\varphi - \varphi_0}{\Delta\theta}\right)^{m+1}\right] \quad (3.9)$$

In this equation φ_0 corresponds to the combustion initialization and $\Delta\theta$ is the duration of the combustion.

Detecting the duration of the combustion is the main issue to model the mass burned fraction values. In this thesis, to approximate the duration of the combustion, in cylinder pressure measurements are examined. It is seen that, if there is no combustion, piston is working like a volumetric pump and the pressure change comes from the volume change. If the combustion starts, incylinder pressure measurement shows a sharp increase and this information helps detecting combustion duration.

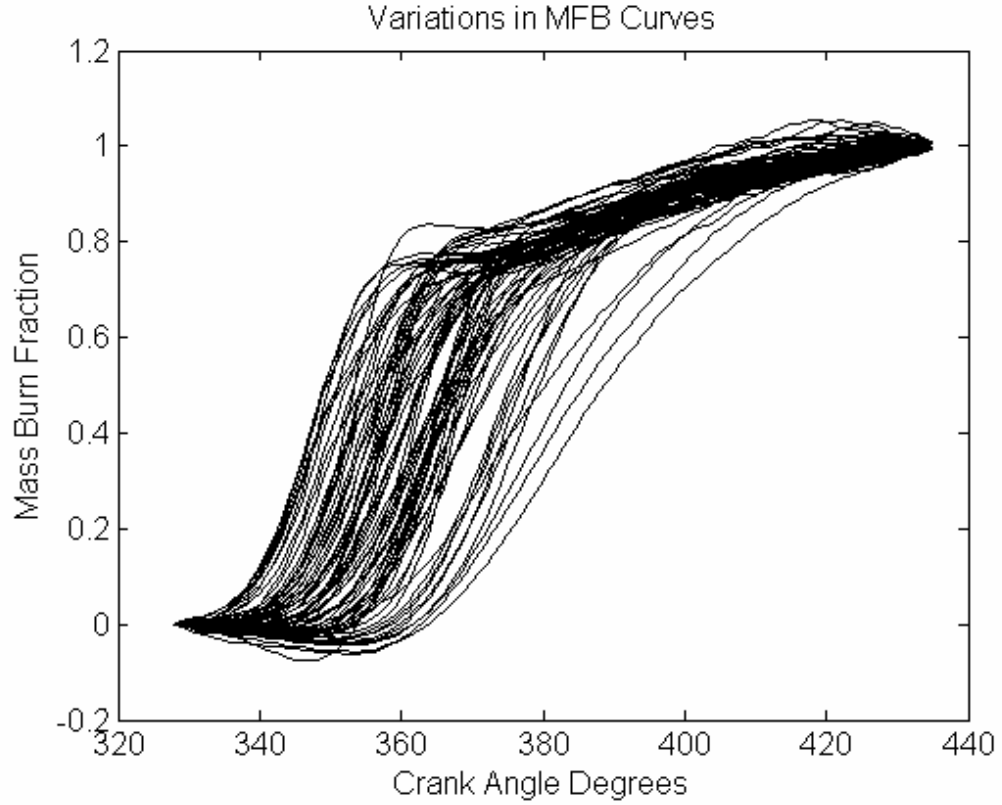


Figure 3.4 : Mass burned fraction variations in gasoline engines [20].

If we little bit discuss on the Figure3.4 found from the literature [20], it could create valuable solutions for our problem. As can be sen from the figure above the start of combustion varies with crank angle for different operating points. On the other hand, the value of end of combustion is almost around 435 crank angle. This means that the end of combustion is almost constant for engine operating points.

In this thesis, the Wiebe function aproximation has ben used for calculations of % 50 mass burned values. On the other hand validity of the Wiebe function aproximation has to be questioned. For this purpose mass burned fraction values are calculated by 2 different methods. The second mentioned method is developed by Rassweiler and Withrow [25]. They claimed that , during combustion, the pressure change Δp , consists of two parts, pressure change because of combustion Δp_c and pressure change because of volume change.

$$\Delta p = \Delta p_c + \Delta p_v \quad (3.10)$$

The assumption made here is that, the pressure change in the Δp_c is directly proportional to the heat realease rate. With the help of this, a cylinder based formulation is derived for mass burned fraction analysis.

To calculate the mass burned fraction, end of combustion (EOC) and start of combustion (SOC) are the most important variables in the equation (3.11). Therefore analyzing the pressure data will clarify the timings of these variables.

$$MFB(\phi) = \frac{\sum_{\phi_{SOC}}^{\phi} \Delta p_c}{\sum_{\phi_{SOC}}^{\phi_{EOC}} \Delta p_c} \quad (3.11)$$

In our case we have the Δp and Δp_v is given with the below equation;

$$\Delta p_v = p_{i+1} - p_i = p_i \left[\left(\frac{V_{i+1}}{V_i} \right)^n - 1 \right] \quad (3.12)$$

p_i is the first pressure value of the recorded cylinder pressure data.

As can be seen from the Figure 3.5, start of main and pilot injections occur at 351 and 349 crank angles according to the ECU measurement. As can be seen from the Figure 3.5, at 372 crank angle, pressure starts to increase, this shows that, due to the combustion start, heat is released into the cylinder and by the increase of in cylinder temperature, proportionally in cylinder pressure increased.

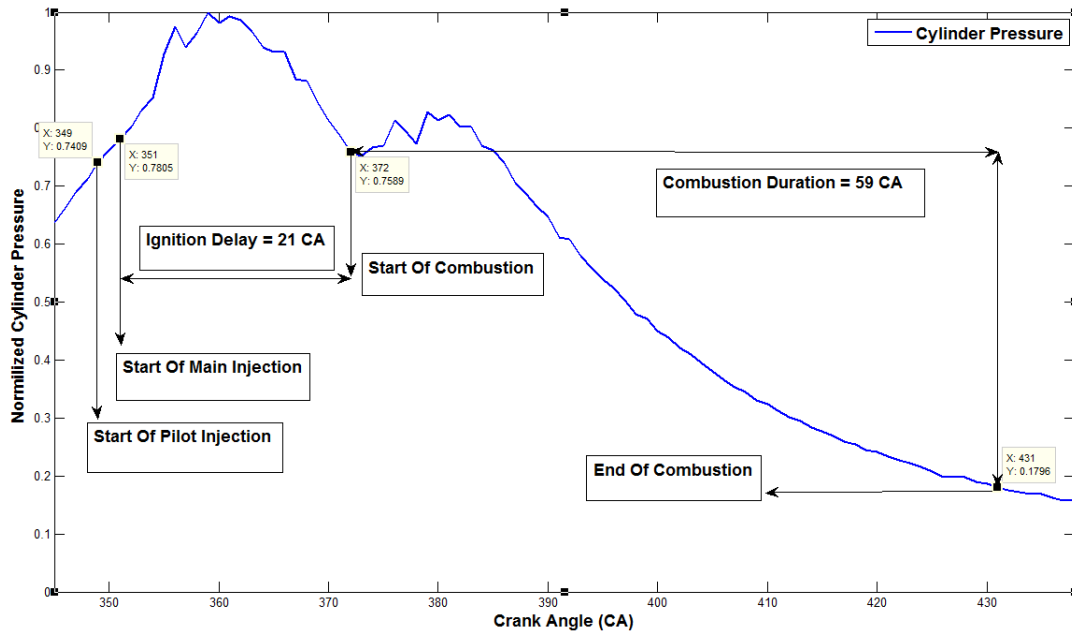


Figure 3.5 : Normalized cylinder pressure at at 2200 rpm and 131 N.m load.

This inference comes from the well known ideal gas assumption. The start of combustion occurs with a delay of 21 crank angle after the injections. To find the end

of combustion, derivative of the cylinder pressure data is also illustrated,. Please see the Figure 3.6.

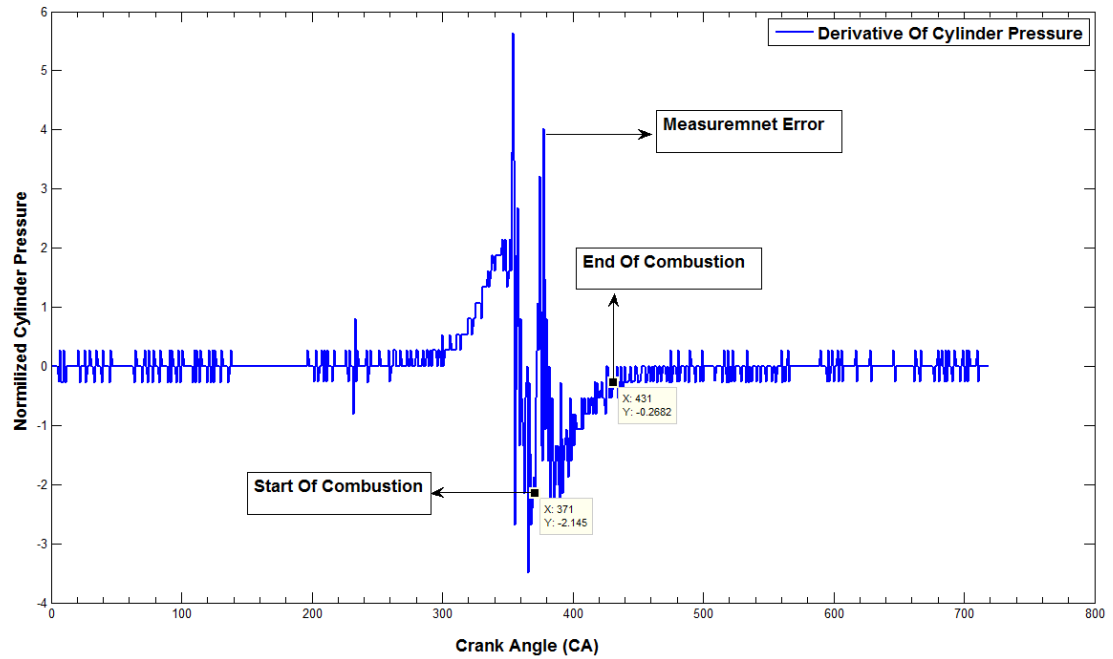


Figure 3.6 : Illustration of EOC from the derivative of cylinder pressure.

If we remember the equations Δp_v term is negative after the top death center, and during the combustion Δp_c is a positive value. If $\Delta p_c > \Delta p_v$ than we will see an increase in the total cylinder pressure change Δp as at the 371- 372 crank angle. The indicator of the end of combustion is the sharp increase of the cylinder pressure as observed after the crank angle 371. This increase continues upto 431-432 crangles. than the rate of change of the pressure aproximately constant because the heat release finished.

To support our assamptions similar analysis have been found from the literature [26]. In the Figure 3.7 an appearent heat release analysis has been applied by the authors. It seems that the heat release proceeds aproximately 65 CA after the combustion start.

Our data shows that, even if the combustion start changes, the combustion finish is aproximately around the 435 crank angle. To simplify calculations, combustion end will be accepted as 435 crank angle. Furthermore, to simplify the calculations, ignition delay will be accepted as 21 crank angle after the main injection. With these simplifications combustion duration $\Delta\theta$ is calculated with the following equation (3.13).

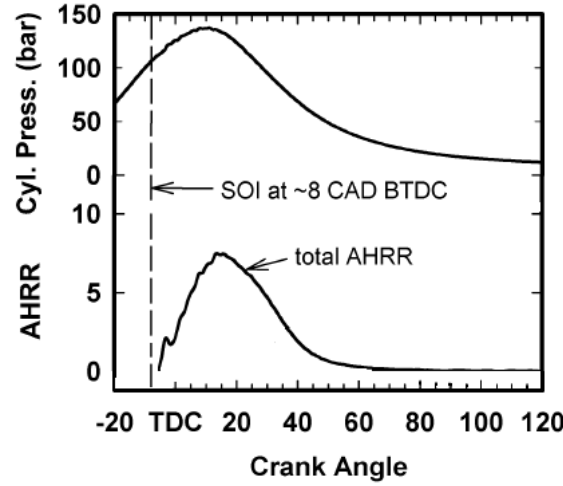


Figure 3.7 : Apparent heat release rate and cylinder pressure profile [26].

$$\Delta\theta = 435 - (StartOfMainInjection + IgnitionDelay) \quad (3.13)$$

Moreover, because we are trying to find the crank angle of the mass burned fraction inverse of the 3.9 is taken and (3.14) is derived.

$$\varphi_{\%50} = \varphi_0 + \Delta\theta \left(\frac{\log(1 - MFB(\varphi))}{-a} \right)^{\frac{1}{m+1}} \quad (3.14)$$

As a result of mass burned fraction calculations, two methods are compared in the Figure 3.8.

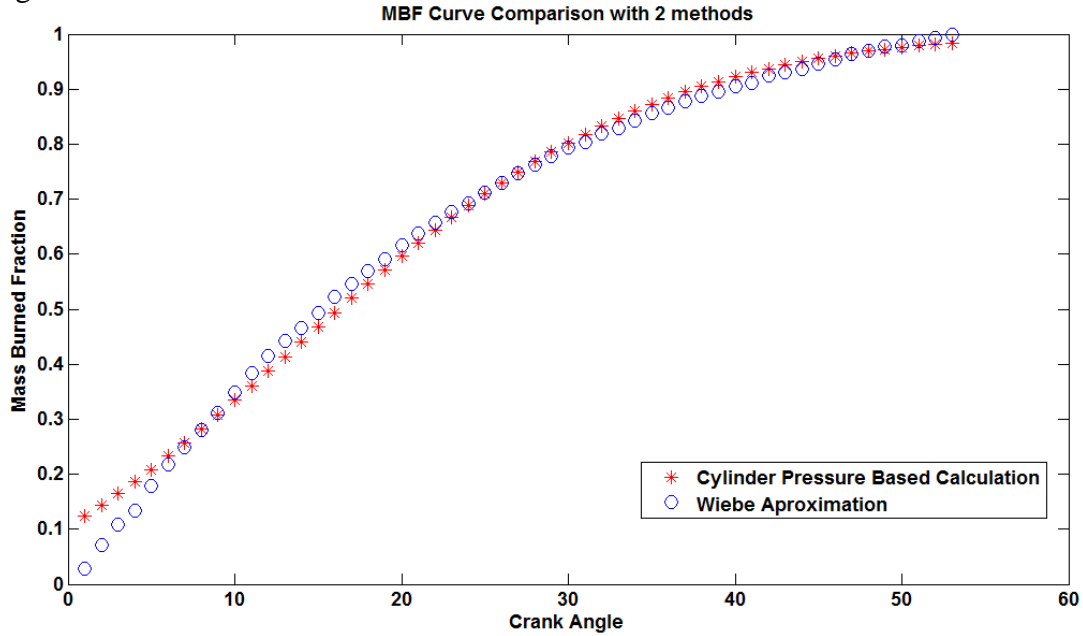


Figure 3.8 : Comparison of methods given in equations (3.9) and (3.11).

First of all, mass burned fraction values are calculated with appropriate equation. Then the best fitting coefficients of the Wiebe functions are calculated by using the NLINFIT function of the MATLAB. If we looked to the Figure 3.11, distribution of

the 'm' values can be found. In this thesis, ' $m = 1.5$ ' will be used in the calculations. Moreover, the distribution of the 'a' values that best fits to the related equation are given in Figure 3.12. In this thesis, ' $a = 2.5$ ' will be used in calculations.

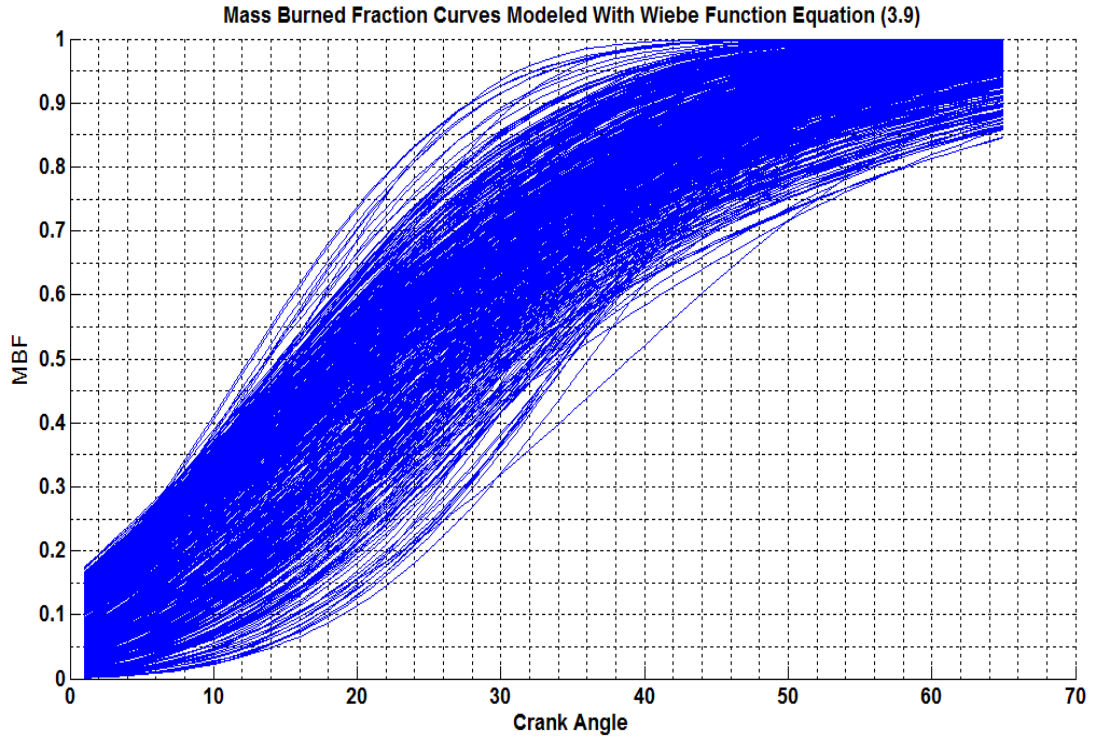


Figure 3.9 : Modeled mass burned fraction with Wiebe approximation.

The modeled mass burned fraction curves with Wiebe approximation is calculated. If we looked to the edge of the curve, because of our assumptions made for the start of combustion, end of combustion and ignition delay , the edge of the curves are like cutted. Because the focus of our modelling is calculation of the center of combustion. It is seen that, two methods approximated the combustion center very close. This is not a problem for our case.

While modeling mass burned fractions, the main problem is the noisy cylinder pressure measurements. In our approximations, we have used the cylinder pressure measurements to approximate the actual mass burned fraction values. Then the Wiebe function coefficients are fitted according to actual mass burned fraction values. The main advantage of the Wiebe approximation is that it does not requires the cylinder pressure as the input. In this thesis, it is puposed to support the inputs of the combustion model from a mean value engine model. In the literature, it is seen that the many of the mean value engine models do not include the crank angle based cylinder model.

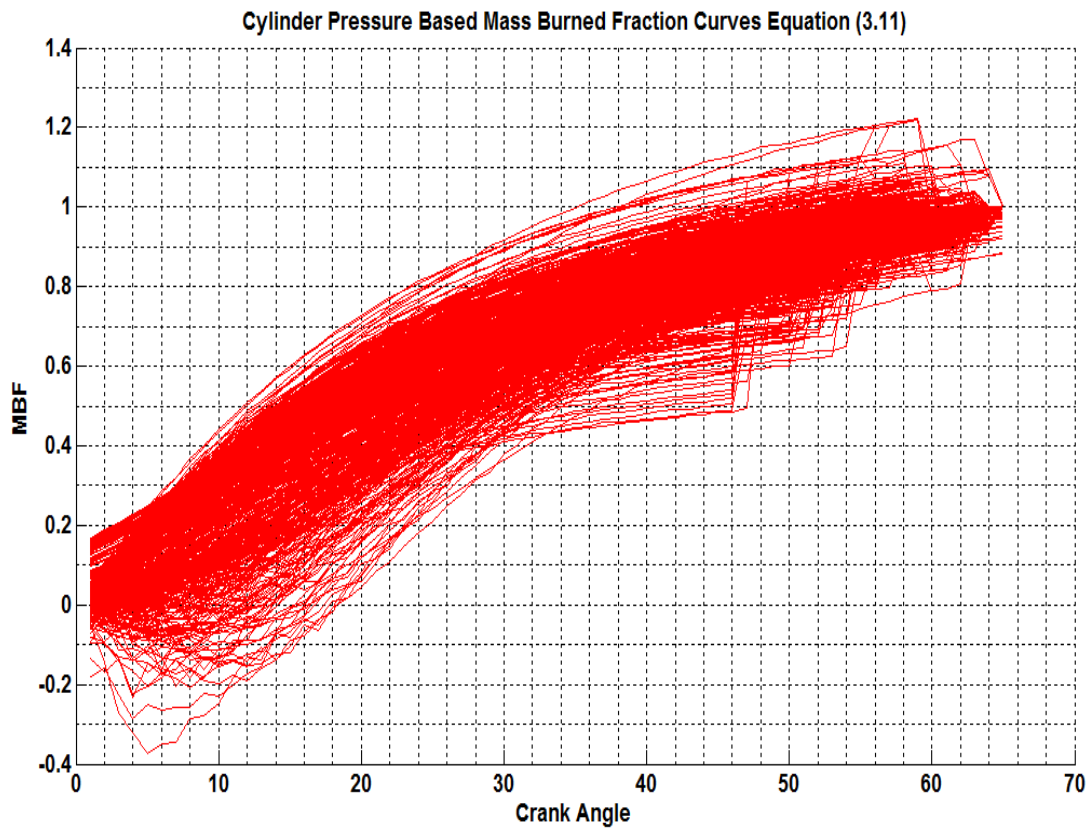


Figure 3.10 : Cylinder pressure based burned mass fraction curves.

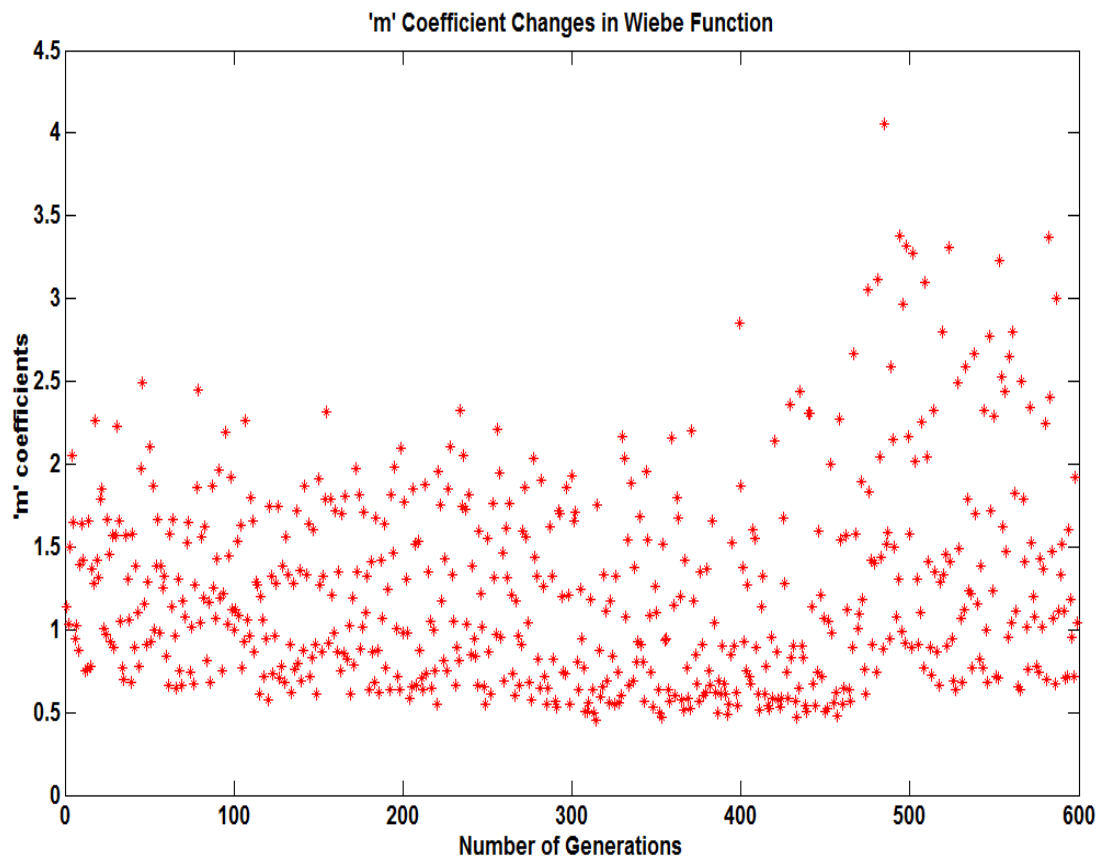


Figure 3.11 : 'm' coefficients that best fitting the Wiebe function to the (3.11).

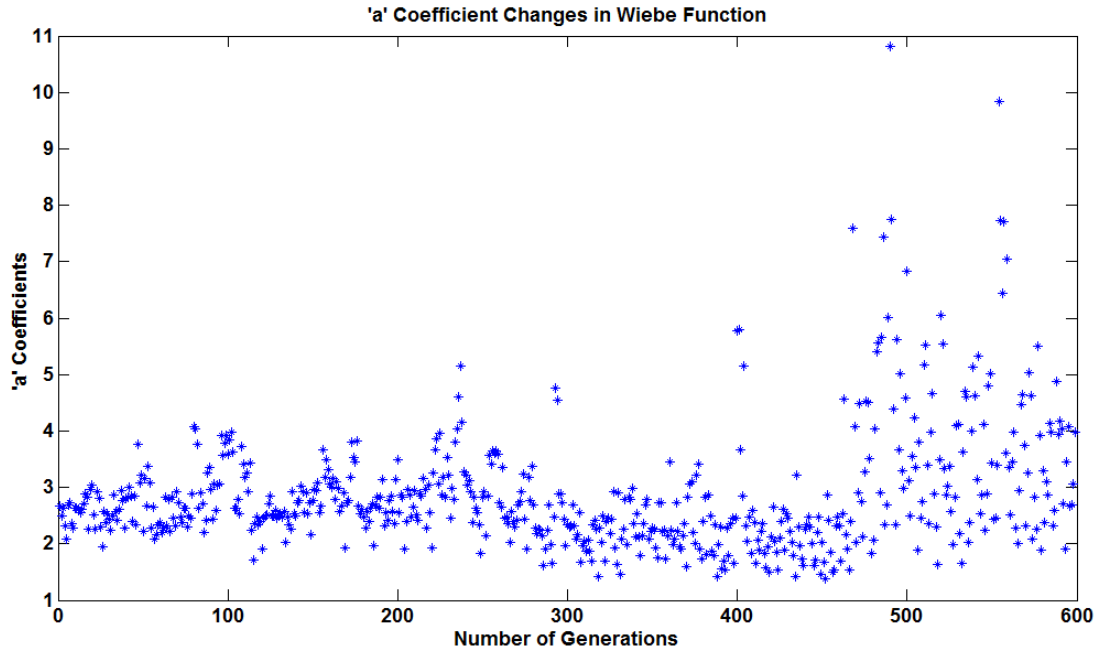


Figure 3.12 : 'a' coefficients that best fitting the Wiebe function to the (3.11).

3.2 Polynomial Based Regression Approach

As a second estimation method polynomial based regression approach has been applied. The need for this method comes from the warning about the accuracy and reliability of symbolic regression approach. There are many disadvantages of the symbolic regression approach that is experienced in this work. The generated equations are not repeatable and convergence of the tuning takes much time when the tree size increases. Moreover, because the generated equations are highly nonlinear, it can cause inaccuracy during the transient testing. Because of these disadvantages and unsatisfied results observed during the validation tests, polynomial based regression approach is also applied in this thesis. In the results section comparisons of the 2 methods are given in detail.

In this application, a switch case modelling method is applied to better model the idle case of the engine operating mode. This is an inference coming from the previous section. The delay part is only an approximation for sensor delays coming from the transient testing. If we looked our model inputs intake manifold pressure and air mass flow is measured values from ECU. The delays of the system can be summarised with the following delays;

- Mass air flow sensor and transportation delays, Manifold absolute pressure sensor delay, rail pressure sensor delay, NOx and PM sensors delays.

Polynomial regression parts given in Figure 3.13 is modeled with steady state measurement points. The delay part is modeled with the first 1000 points of the WHTC test, on the other hand validation task carried out for 18000 points which is the whole operating range of the transient test WHTC.

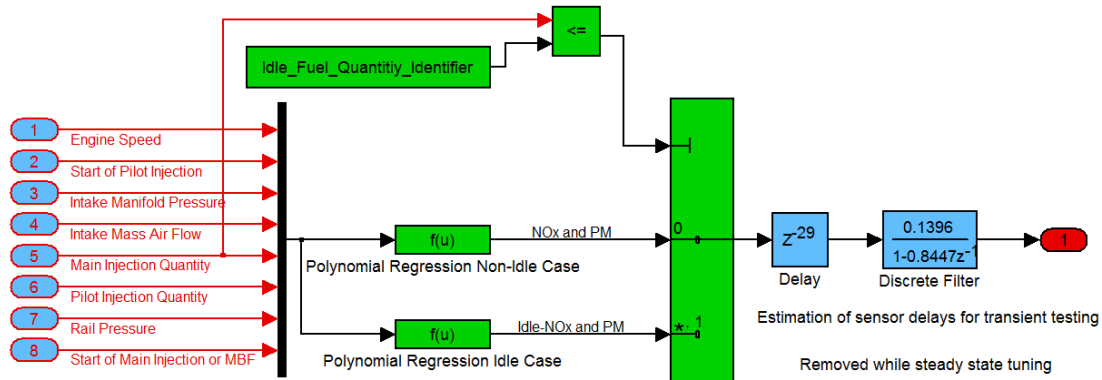


Figure 3.13 : Model structure of polynomial regression.

If we summarise the tuning technique in the following flow chart, it will be more easy to understand the modelling approach.

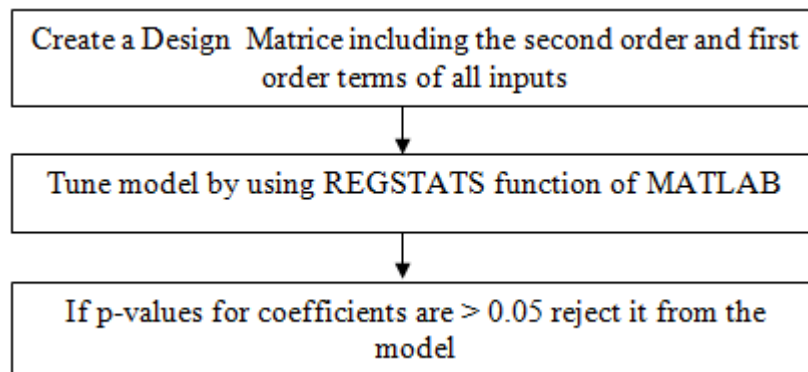


Figure 3.14 : Flow chart of the polynomial based regression approach.

4. RESULTS AND DISCUSSION

Results of the emission modeling methods are given in this section. Moreover detailed discussions are carried out on the results.

Table 4.1 : Overall Results.

Modeling Method	R Square	
	PM	NO _x
Symbolic Regression with base map with %50 MBF	0.369	0.705
Symbolic Regression with base map with SOI Main	0.261	0.597
Symbolic Regression without base map with SOI Main	0.161	0.708
Polynomial Regression Approach	0.74	0.8272
WHTC Validation Results with Polynomial Approach	-	0.8291
WHTC Validation with Mean Value Engine Model	-	0.685
WHTC Validation with Mean Value Engine Model and 2nd Calibration	-	0.30

4.1 Results of Symbolic Regression Approach With Base Map

As we explain details of this approach in the previous section, 4 different simulations are carried out and the results of simulations are given below.

The Figure 4.1 shows the base map of the NO_x. The aim of creating this base map was to simulate actual operating response of the engine.

This means for one operating point, injection quantities and timings, set point of mass airflow, manifold absolute pressure and rail pressure are swept around the single operating point. This base map is aimed to simulate the response of the stationary operating points of the diesel engine. Moreover sweeping the setpoint values gives us multidimensional aspects of the engine response. If a model is created such kind of a data, it will be more robust and the simulated results will be more accurate in case of a calibration change.

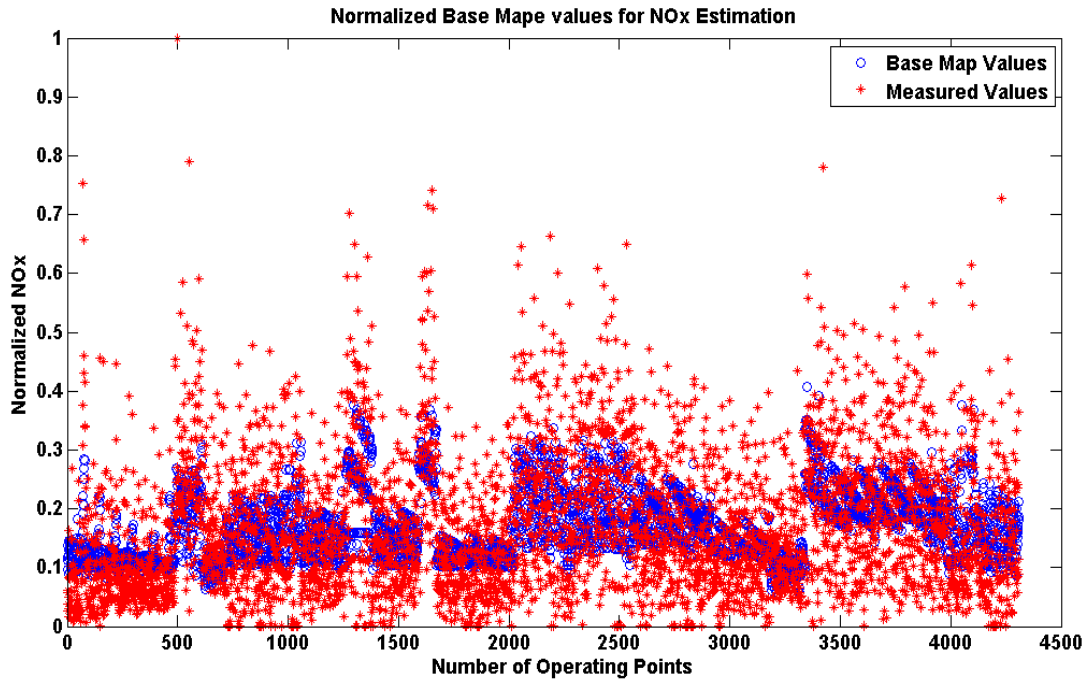


Figure 4.1 : Base map distribution of NOx used in symbolic regression.

In Figure 4.3 and 4.4, the simulation results of the NOx is given. The R square value of the simulation is around 0.7. The mass burned fraction values are used to model NOx in this simulation.

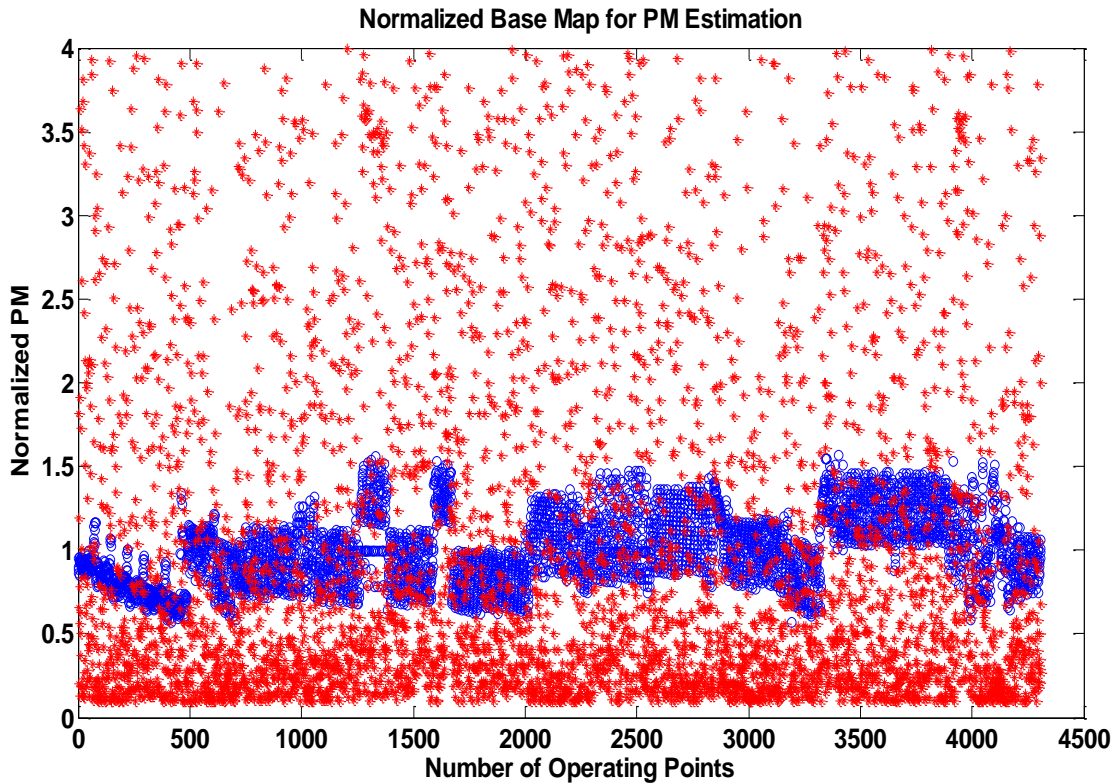


Figure 4.2 : Base map distribution of PM used in symbolic regression.

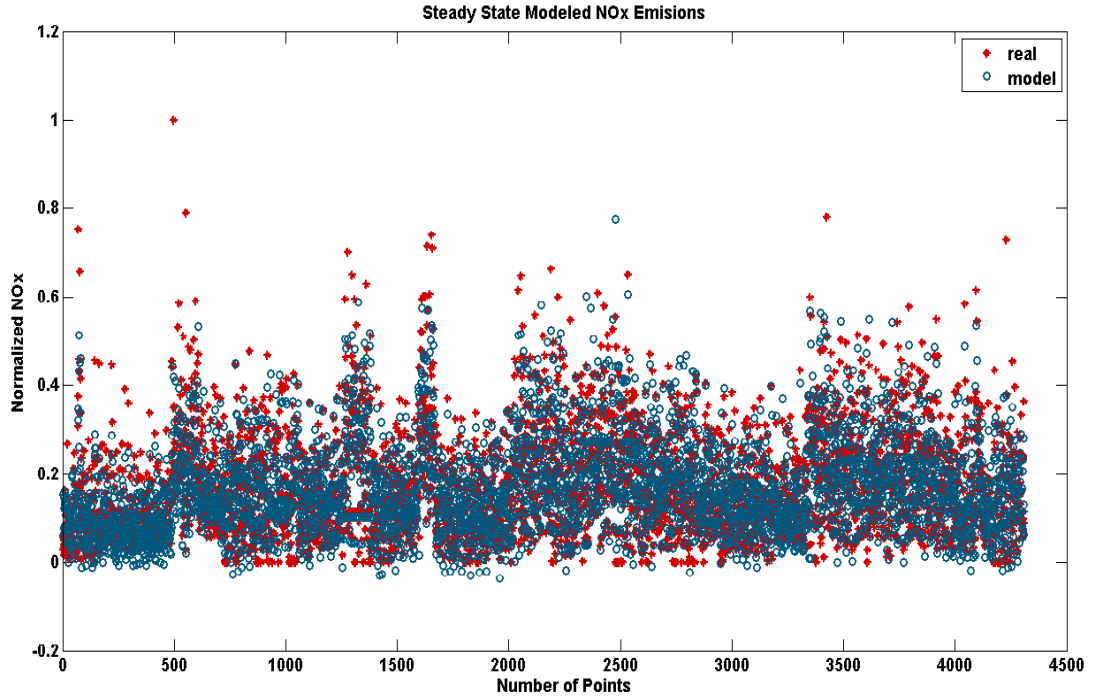


Figure 4.3 : Normalized NOx simulation results with %50 MBF as 9th input.

On the other hand, If we looked to the simulation results of the Figure 4.5 and 4.6, the R square value is around 0.6. From these results, it seems that using the mass burned fraction values increases the accuracy of the simulation. However, it should be notted that, symbolic regression creates random model structures. I can say that , I was expecting to see a drastical increase in the accuracy.

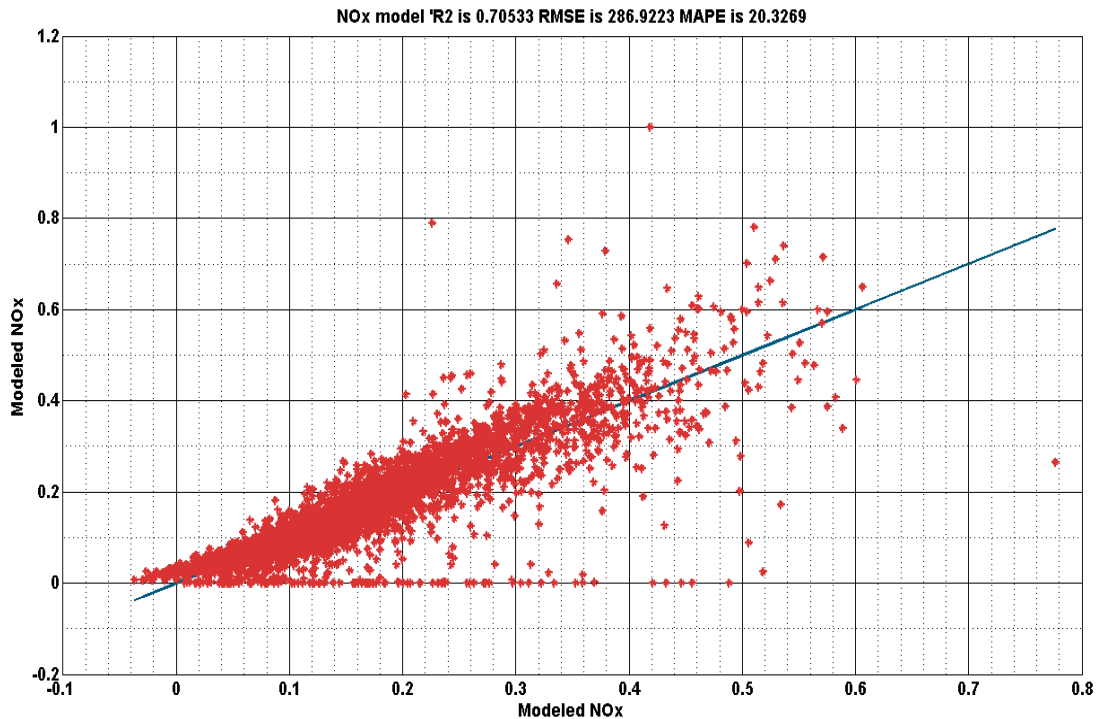


Figure 4.4 : R square results of NOx with %50 MBF as 9th input.

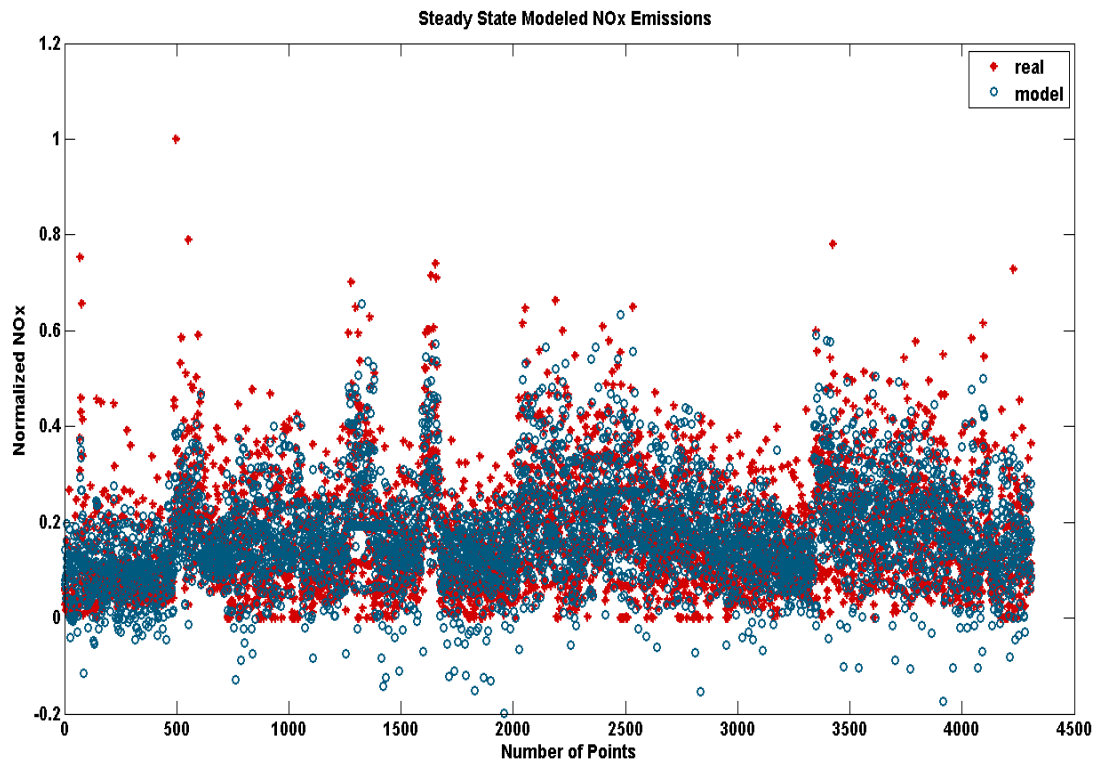


Figure 4.5 : Normalized NOx results with start of main injection as 9th input.

The Figure 4.7 and 4.8 are belong to the simulation results of the PM in which calculations of mass burned fraction is used as the 9th input.

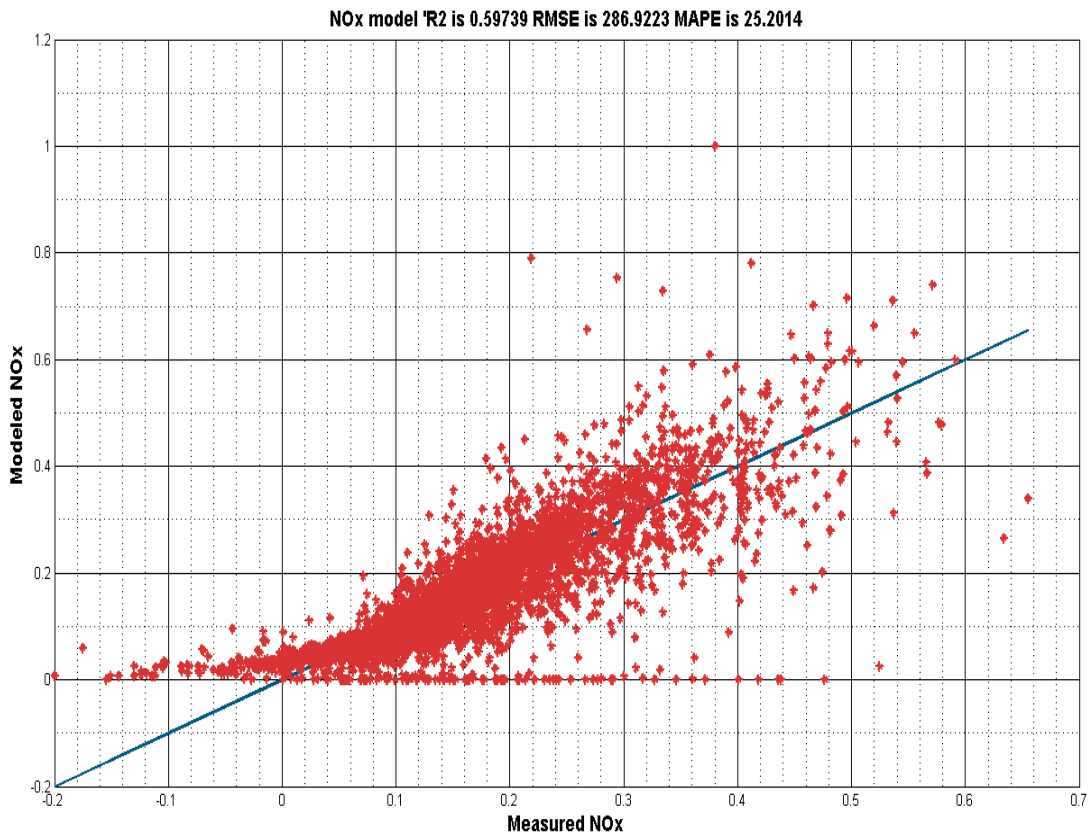


Figure 4.6 : R square results of NOx with start of main injection as 9th input.

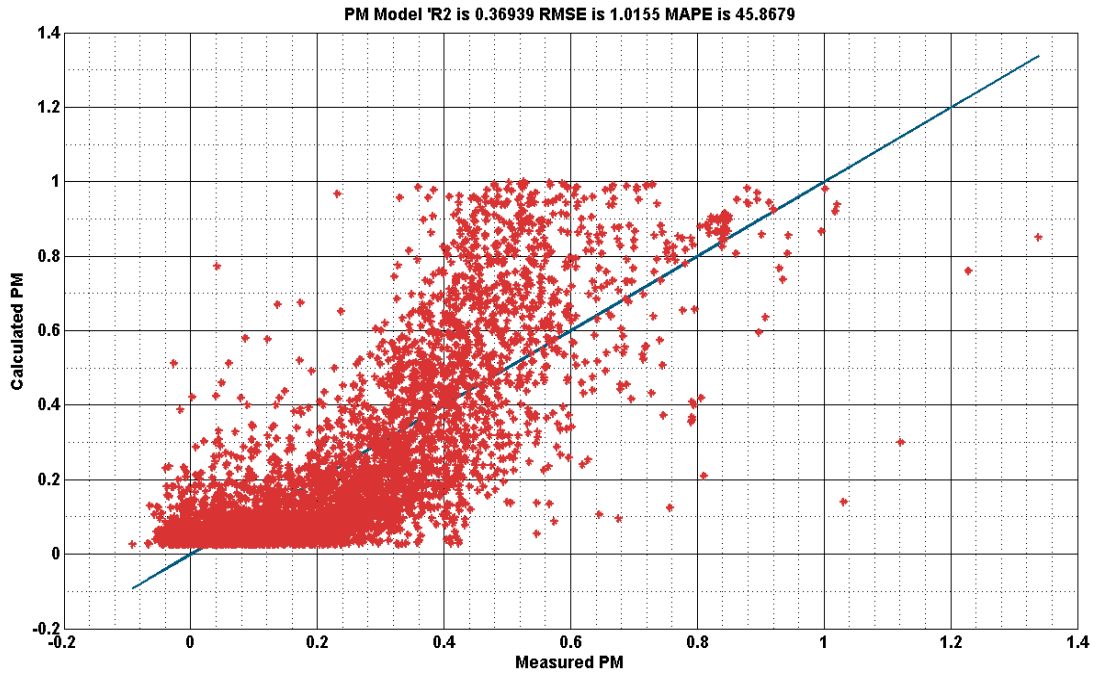


Figure 4.7 : R square results of PM with %50 MBF as 9th input.

On the other hand the Figure 4.9 and 4.10 are simulation results of start of main injection case. The R square values are 0.37 and 0.26 for mass burned fraction and start of main injection cases. If we remember the equation (1.2) given by the Hiroyasu, he claimed that soot formation is increasing with the increase of the mass burned fraction rate. Form these figures Hiroyasu seems right. There is an increase on accuracy but still these estimations are not acceptable to be able to use these models in the control algorithm development or engine calibration processes.

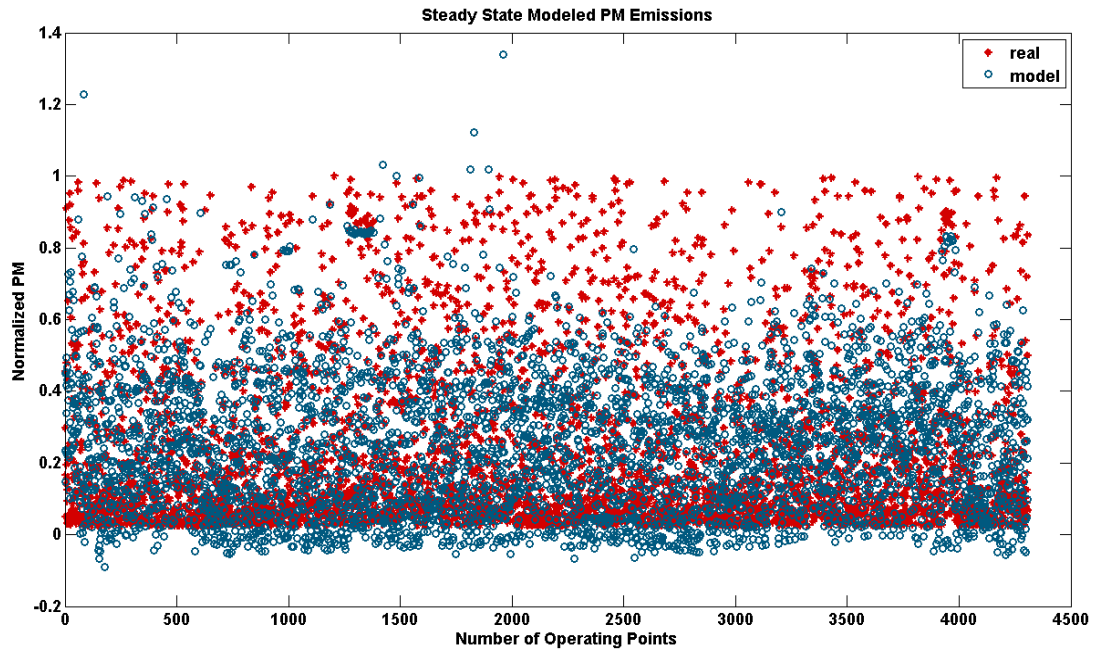


Figure 4.8 : Normalized PM simulation results with %50 MBF as 9th input.

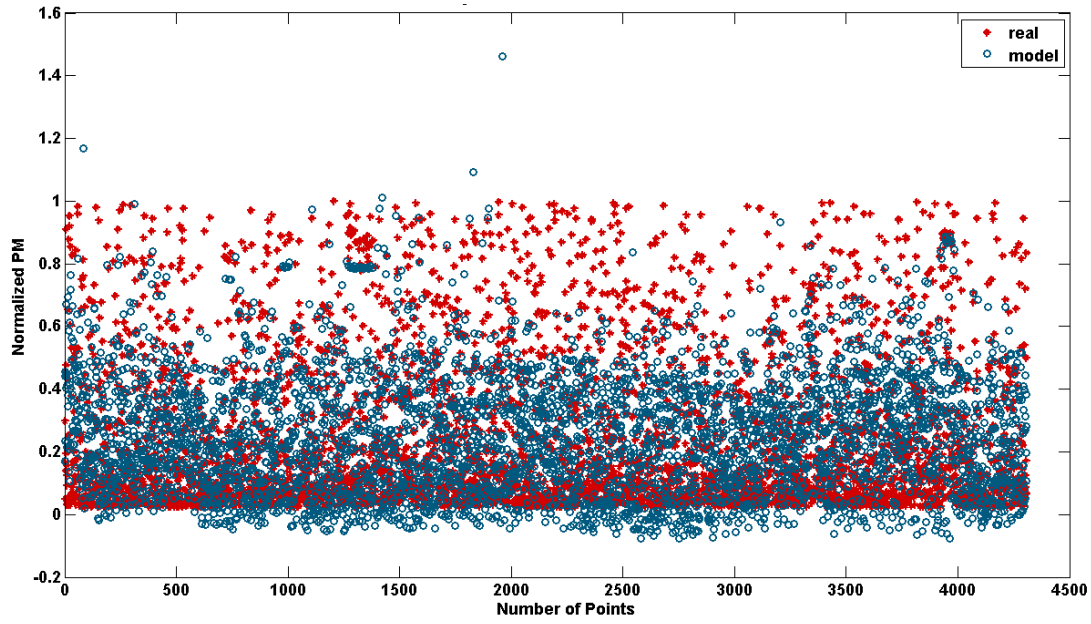


Figure 4.9 : Normalized PM results with start of main injection as 9th input.

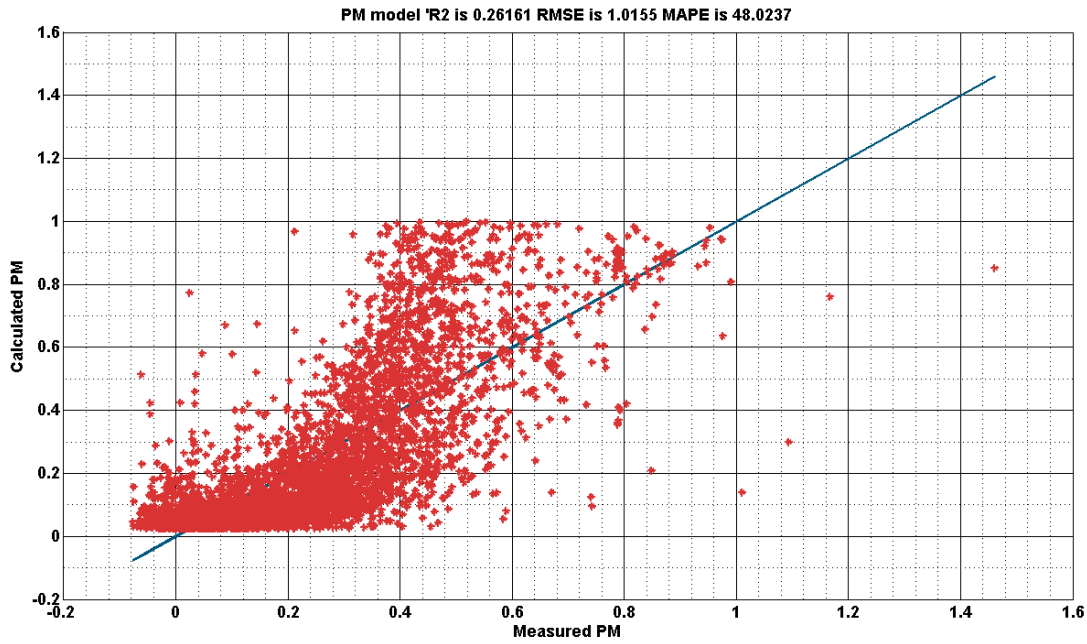


Figure 4.10 : R square results of PM with start of main injection as 9th input.

4.2 Results of Symbolic Regression Approach Without Base Map

To better understand the effect of base map approximation, they are removed from the model structure. Moreover, with these simulations, PM accuracy is reduced while the accuracy of the NOx estimation increasing.

Due to using mass burned fraction or start of main injection shows closer results in accuracy, only the main injection quantity is used in simulations because its

robustness. The values of the main injection timings are more reliable because they are directly measured from the ECU. The results are given in Figure 4.11 and 4.12 for NOx.

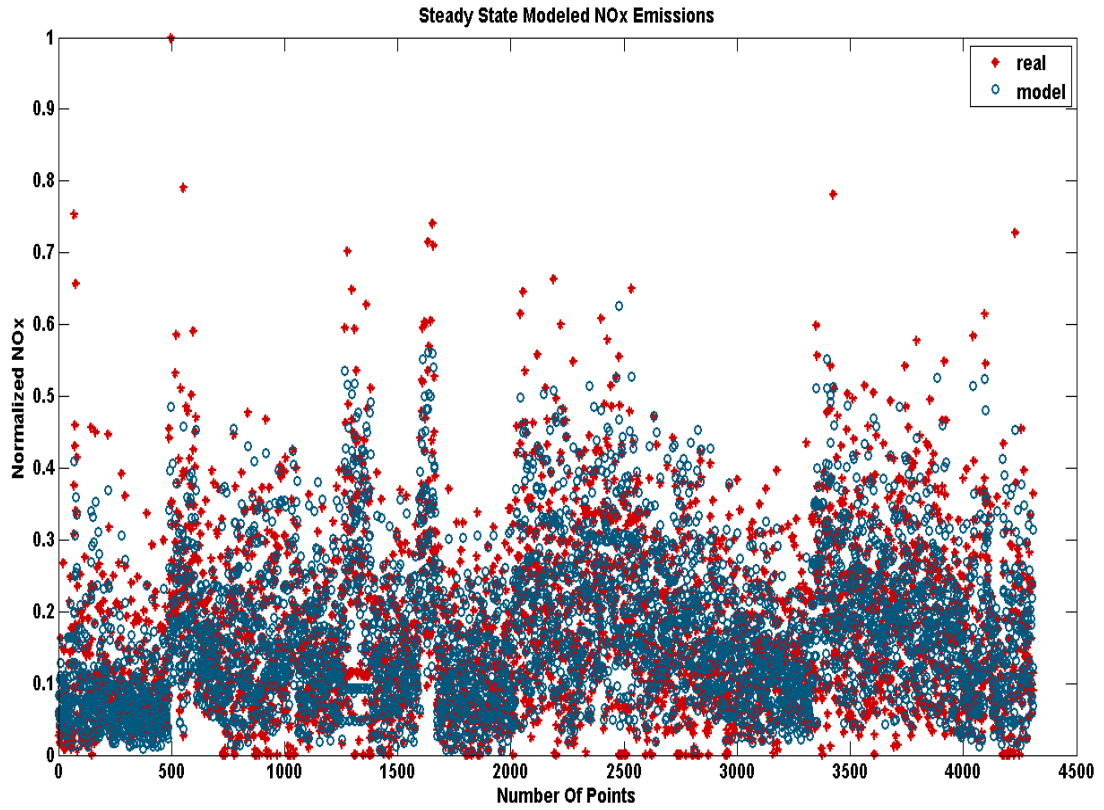


Figure 4.11 : Normalized NOx results with start of main injection as 8th input.

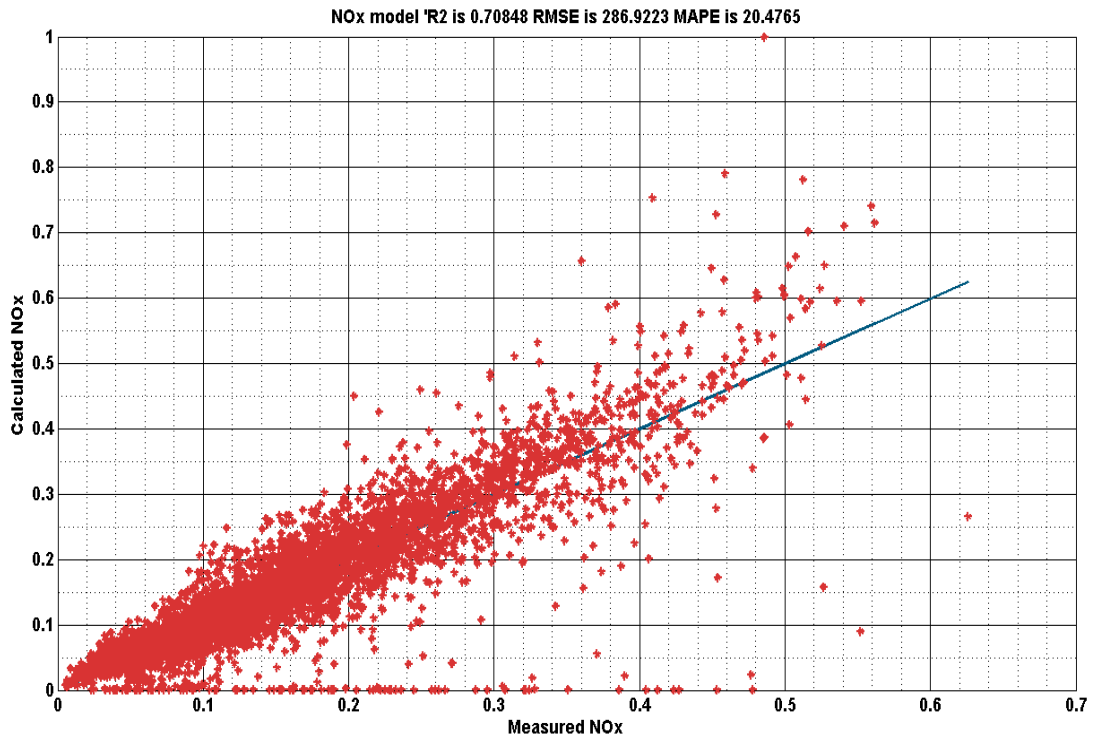


Figure 4.12 : R square results of NOx with start of main injection as 8th input.

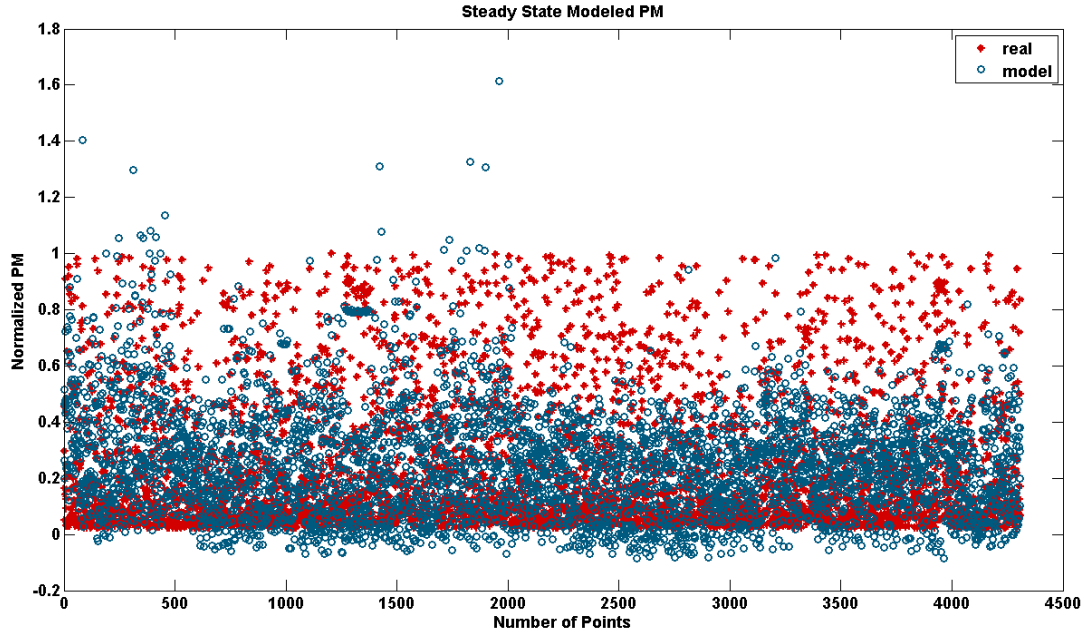


Figure 4.13 : Normalized PM simulations with start of main injection as 8th input.

The R square value for NOx is 0.708. Please remember the r square results of the NOx with %50 MBF as 9th input. Very close accuracy have been achieved by using the mass burned fraction. Actually, this is highly related with our assumptions made in the previous section. Finally, the PM results shows a drastically decrease compared to the previous trainings.

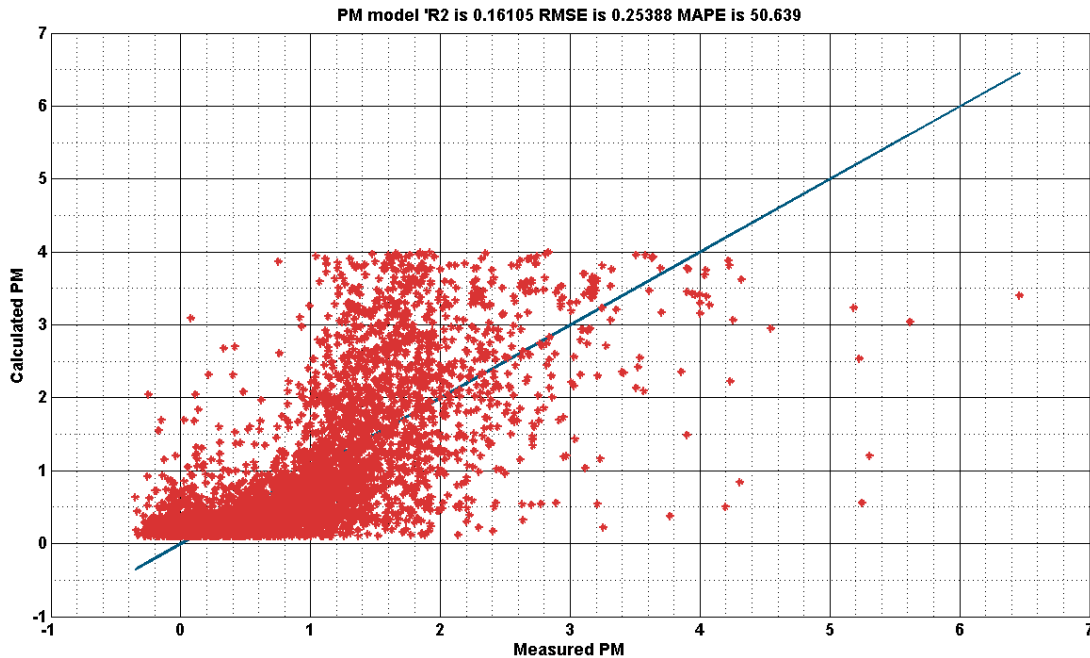


Figure 4.14 : R square results of PM with start of main injection as 8th input.

As result, It is clear that symbolic regression is not a suitable solution for engine emission modelling approaches, because the derived equation structures are highly

non linear and is not repeatable. I want to add also that the GPTIPS does not permits a normal computer to create complicated equation structures. In manual trainings, it is observed that the maximum allowable tree depth is 9 with 7 or 8 multigen options . If you choose more than these, calculations do not stop and computer does not responds any thing.

4.3 Results of Polynomial Regression Approach

Finally, with the application of polynomial based regression, high accuracy and acceptable results achieved on the NO_x and PM results. The main reason getting such kind of high accuracy is the simple structure of the method. With this method, tuning is faster and the derived structure of the equations has 26 coefficients for both idle and normal running cases.

Please focus on the Figure 4.16 and 4.20, the steady state and transient simulation results are highly accurate than the symbolic regression approach.

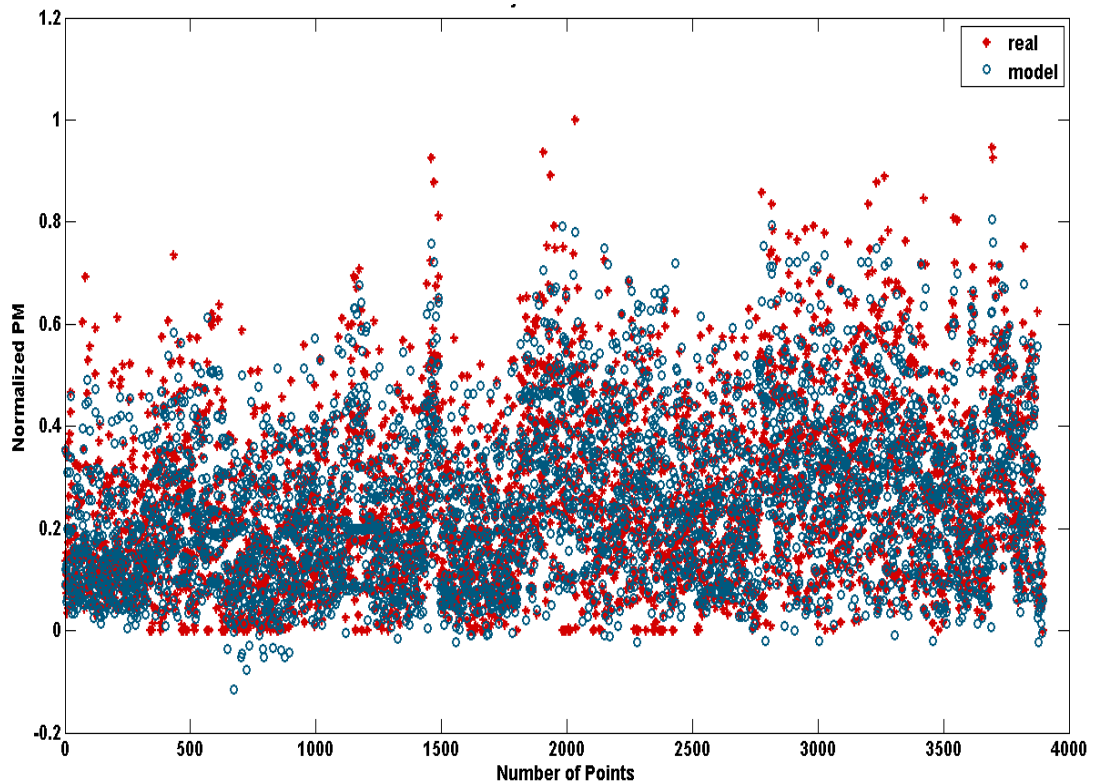


Figure 4.15 : Steady state NO_x results.

In our modeling approach, accuracy is the more important than the precision. The main reason of that is the modeling difficulties. The uncertainties of the combustion event makes harder modeling of it. To have an accurate combustion model detailed

measurements should be taken regarding to incylinder dynamics. As an example, temperature is highly effective on the reaction rates of the combustion event. In the dynamometer utilized in this thesis, has not a temperature sensor. Ususally, an average temperature measurement does not have a meaning for combustion modeling. The NOx and the soot formated at the same time, but in the different temperature zones inside the cylinder. This makes the measurement of the an average in cylinder temperature unnecessary.

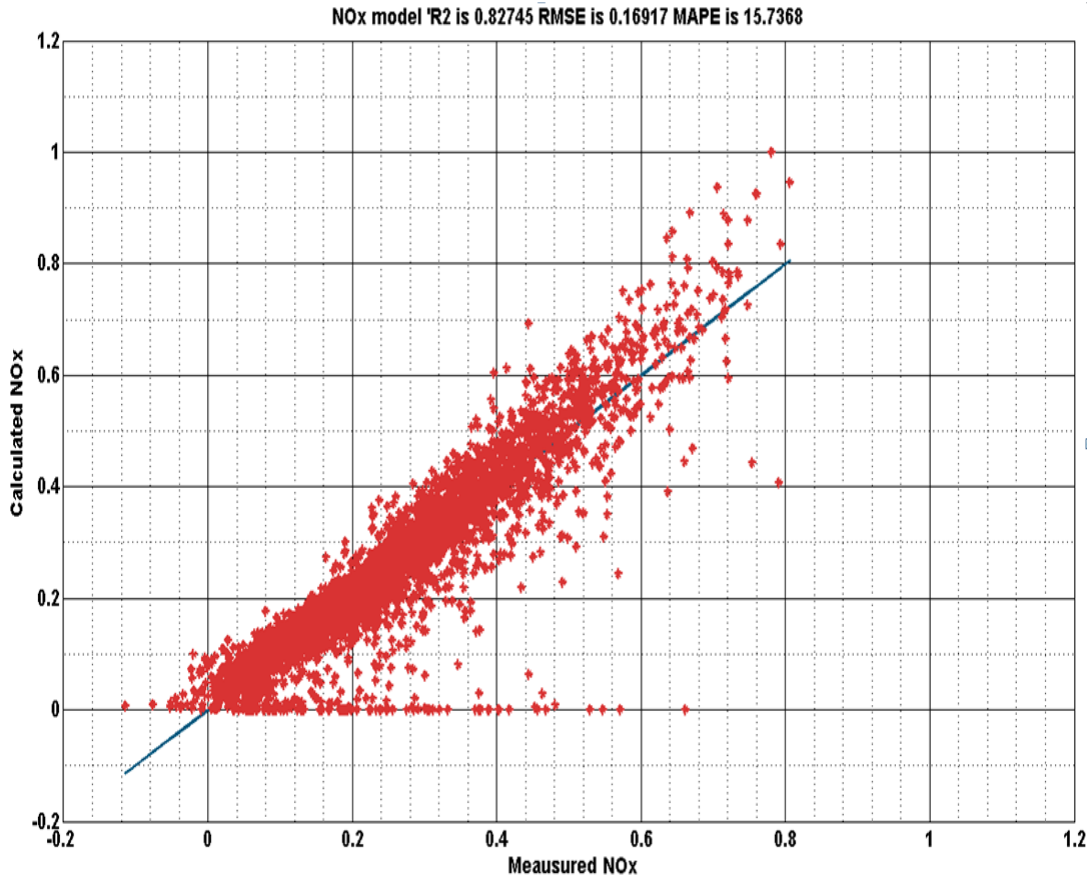


Figure 4.16 : Steady state NOx R square results.

Closer results on the steady state testing and transient testing shows the robustness of the model structure and modelling methodology. Splitting the model in to two parts simplified the problem. In their nature, discountinuous functions and the idle mode of an engine are very similar, because in both case the actual response of the function or engine is really different from the normal operating conditions. Moreover, the delay time aproximation is also increased the transient tracing of the model. The delay observed in the measurements, comes from the sensor delays and from the engine itself. The emission measurements are taken from the output of the turbocharger, while the air flow and pressure measurements are taken before the cylinders.

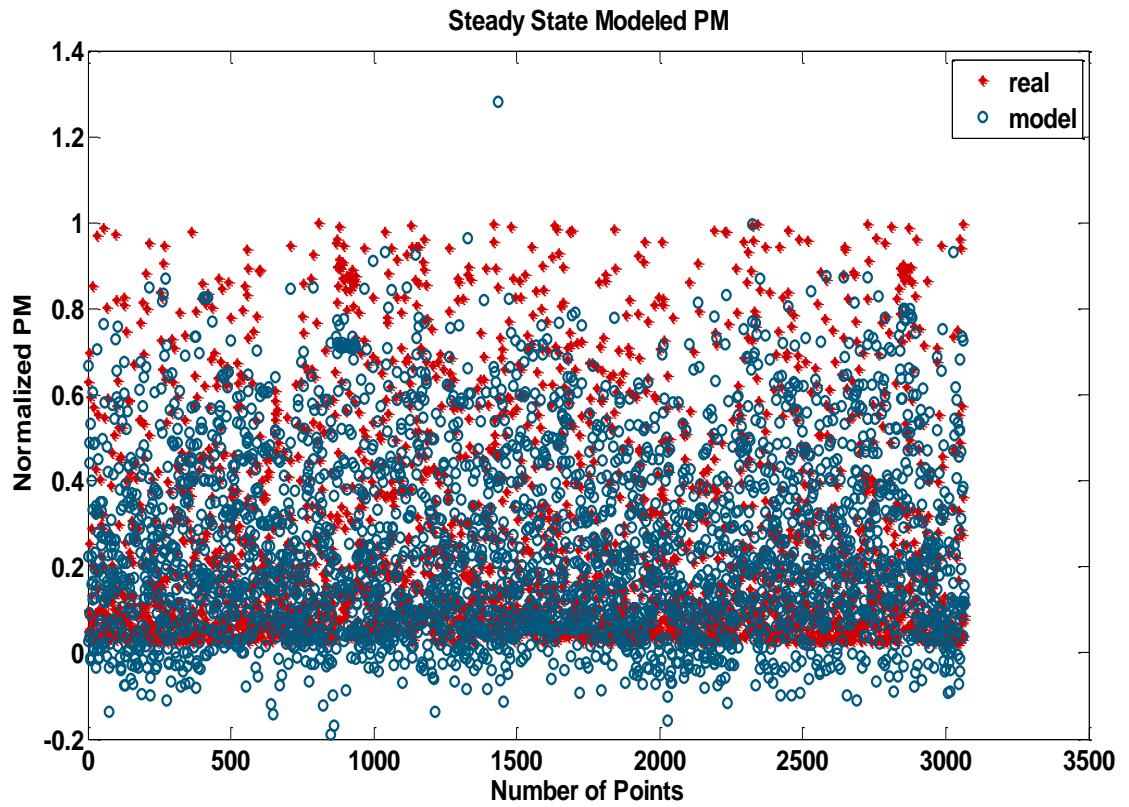


Figure 4.17 : Steady state PM results.

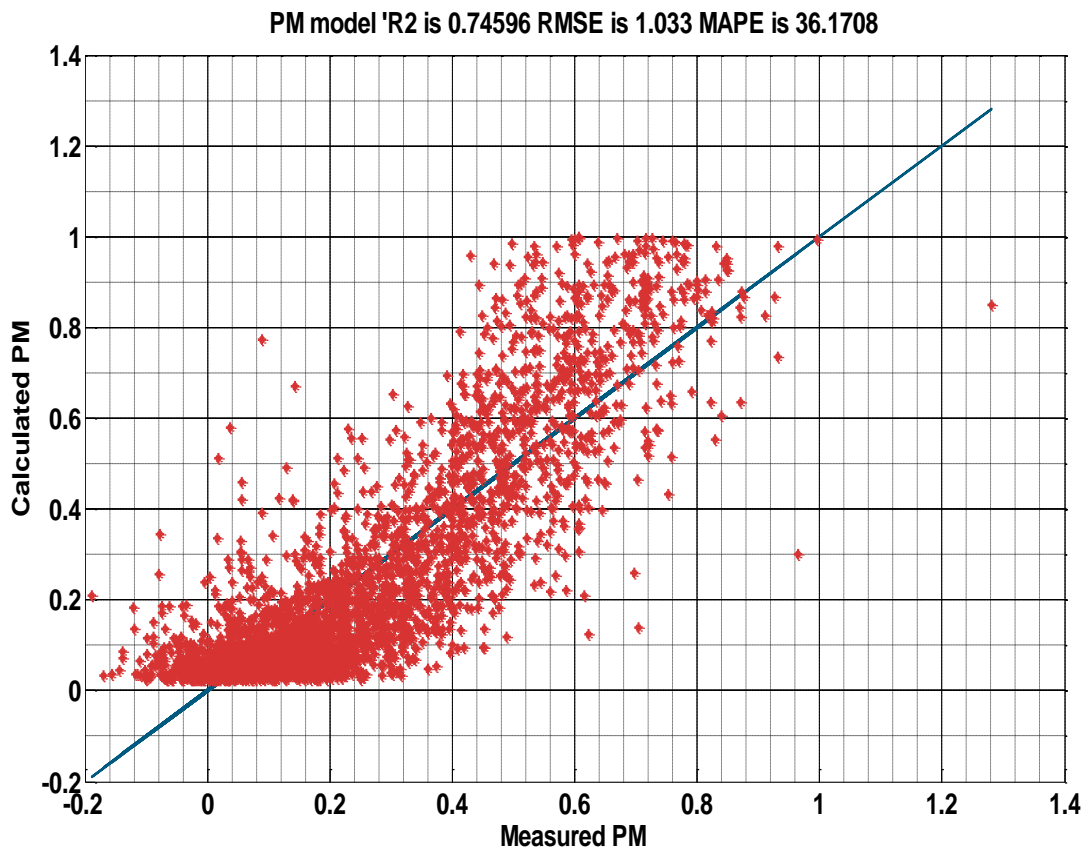


Figure 4.18 : R square results of steady state PM estimation.

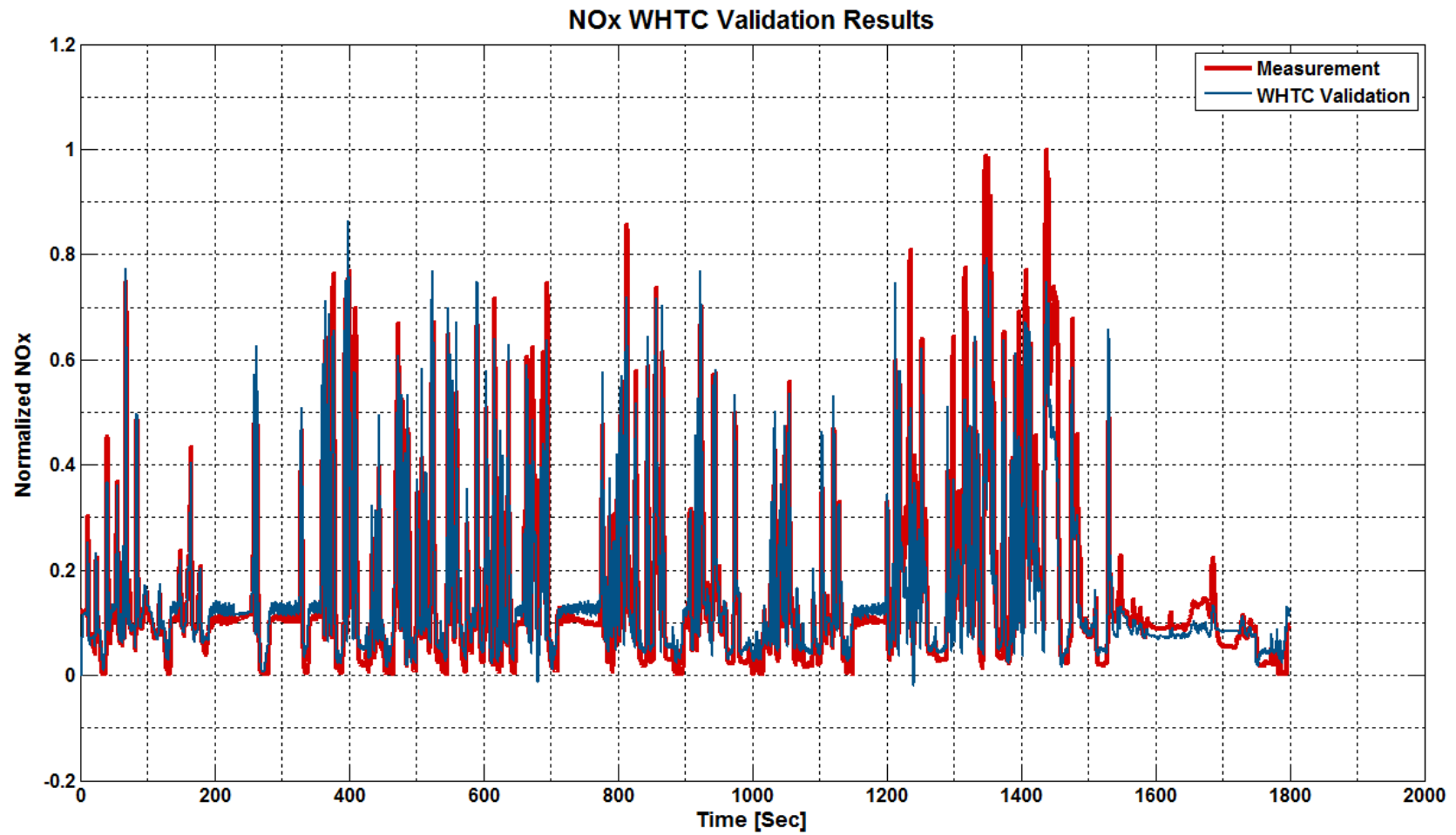


Figure 4.19 : WHTC results of the NOx.

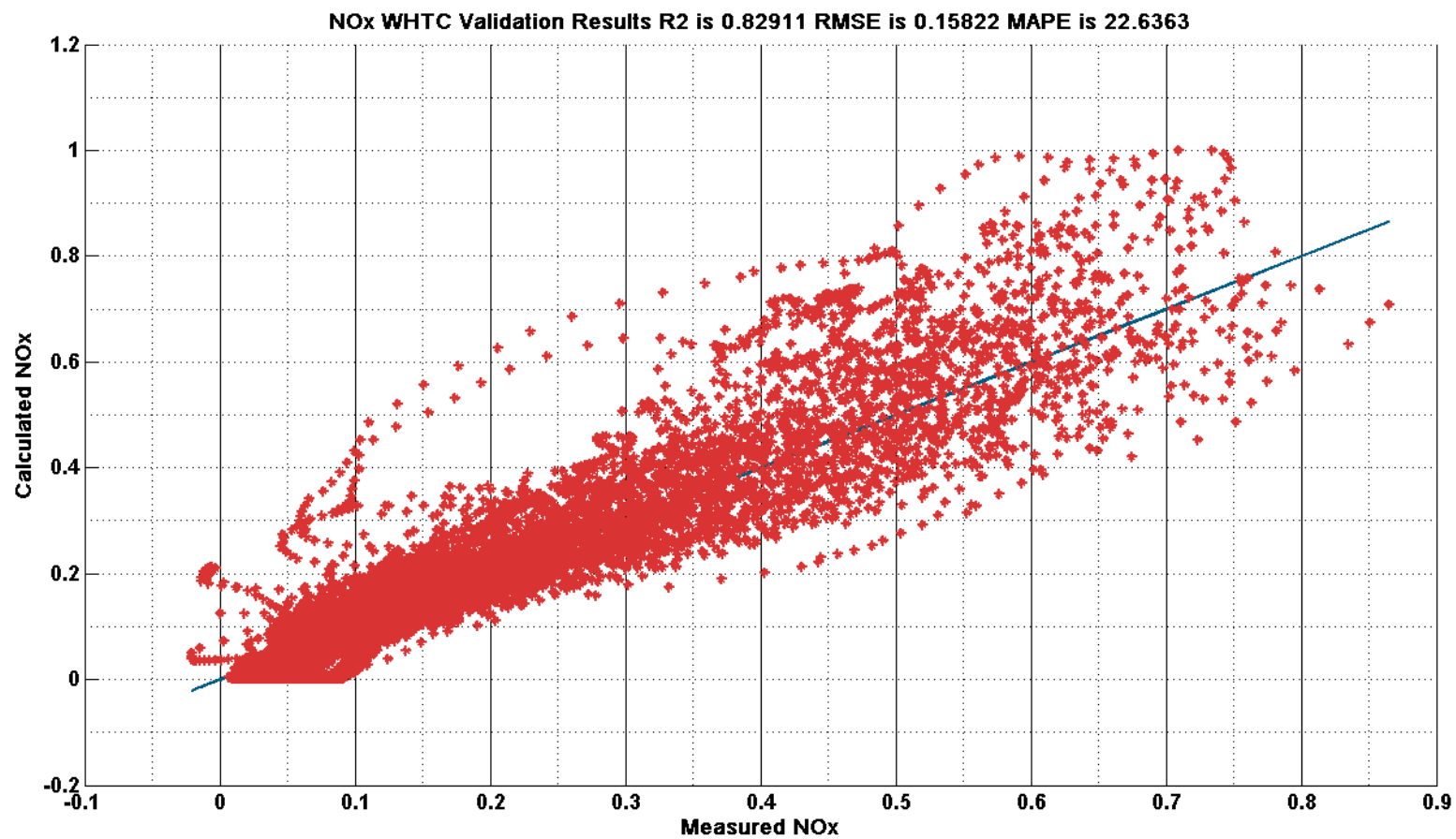


Figure 4.20 : WHTC R square results of the NOx.

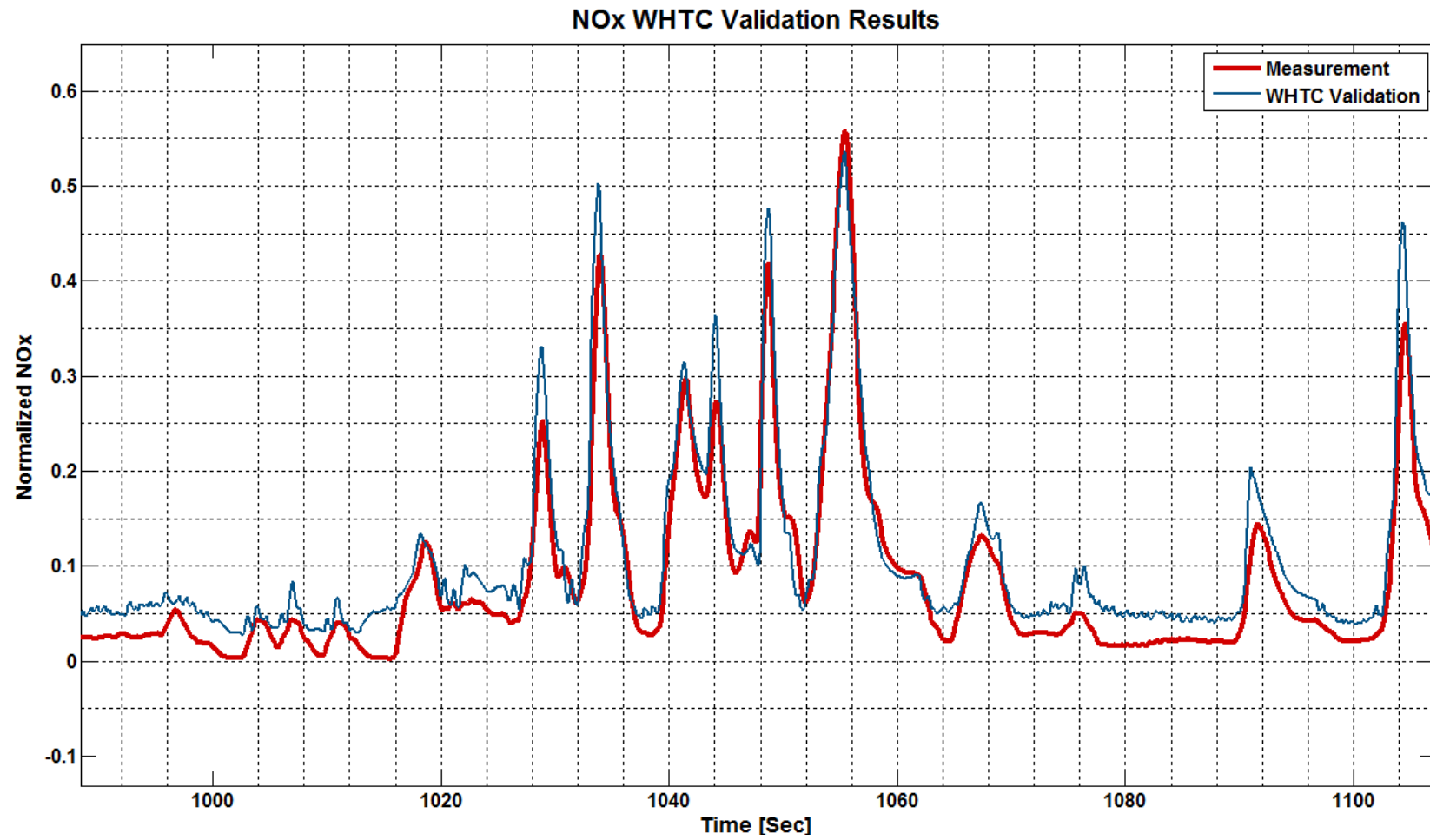


Figure 4.21 : WHTC tracing of the simulated NOx.

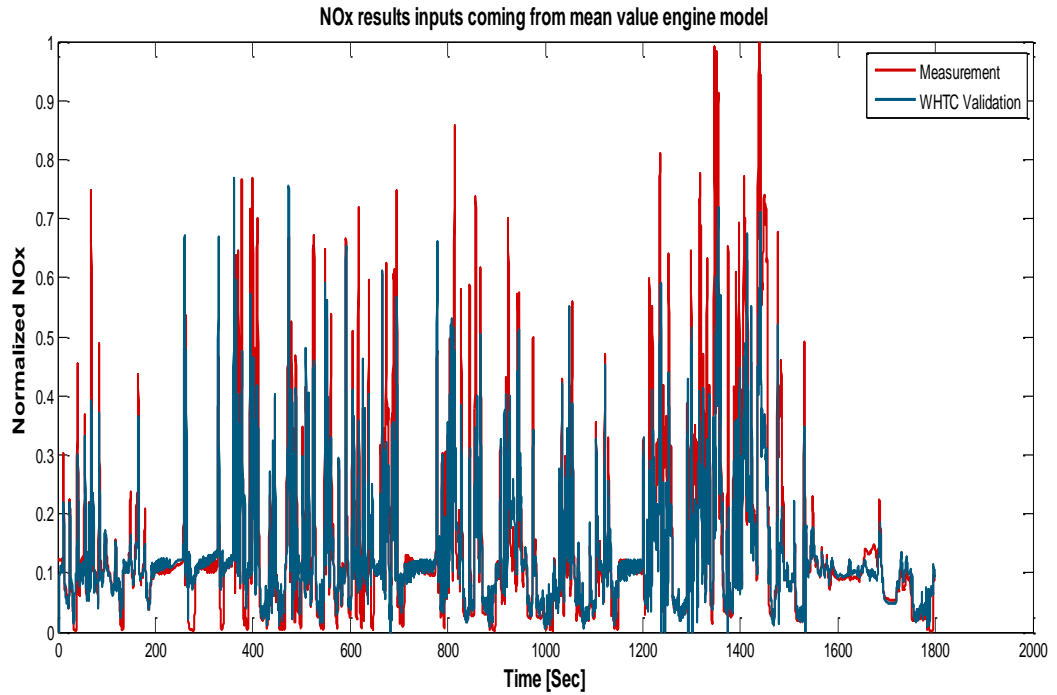


Figure 4.22 : NOx results with mean value engine model [27].

Moreover, the generated emission model is added to the mean value engine model which details are given in [27]. Results show that, the model is able to give an acceptable tracing with the validation data.

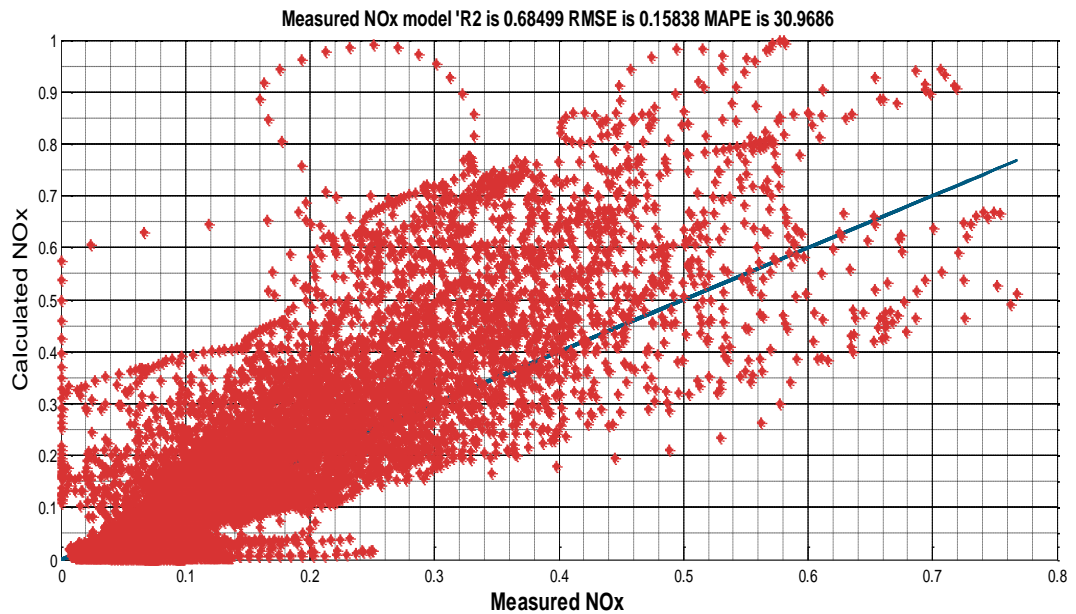


Figure 4.23 : R square results of the NOx with mean value engine model [27].

The below results are belong to a second calibration test. We run a second WHTC test with different calibration and results shows that the generated emission model is capable tracing the NOx values even if a calibration change occurs.

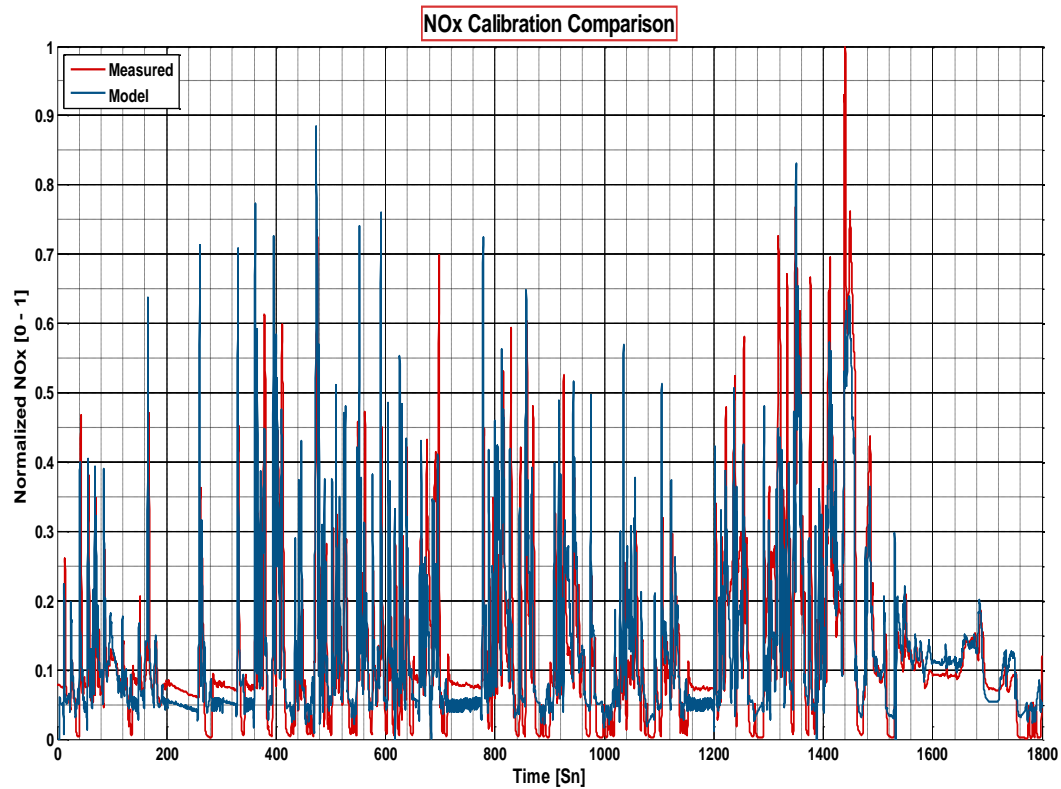


Figure 4.24 : WHTC results with different calibration.

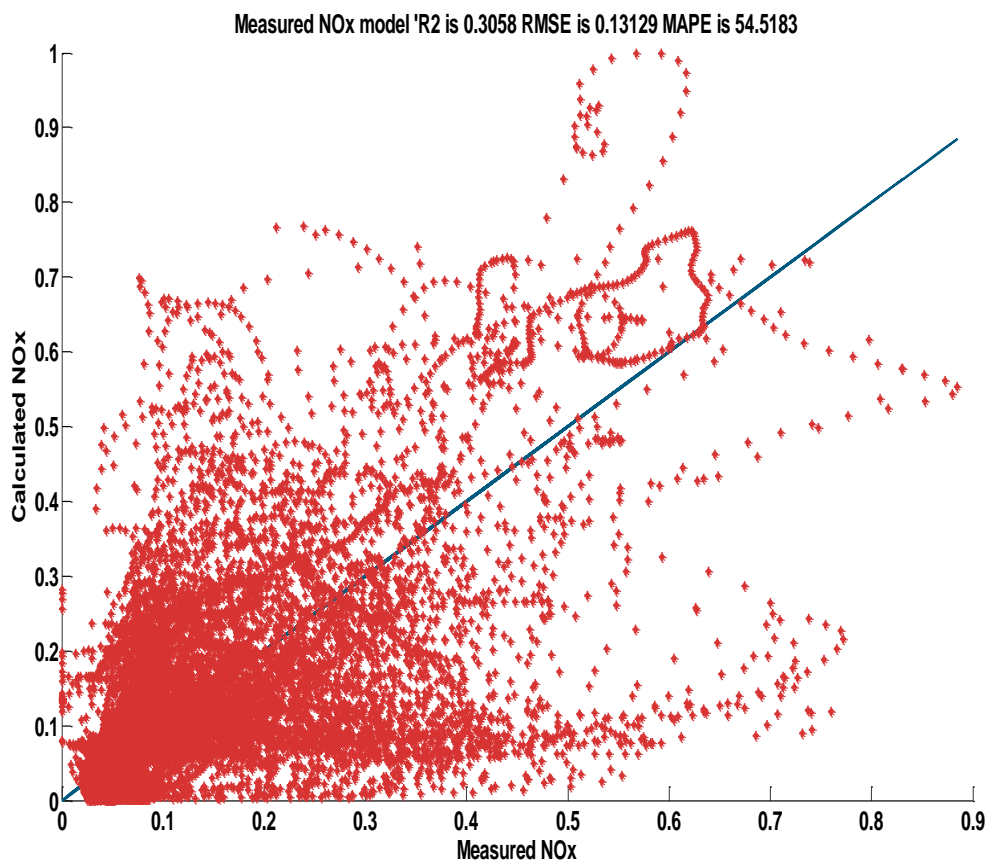


Figure 4.25 : R square results of second calibration validation.

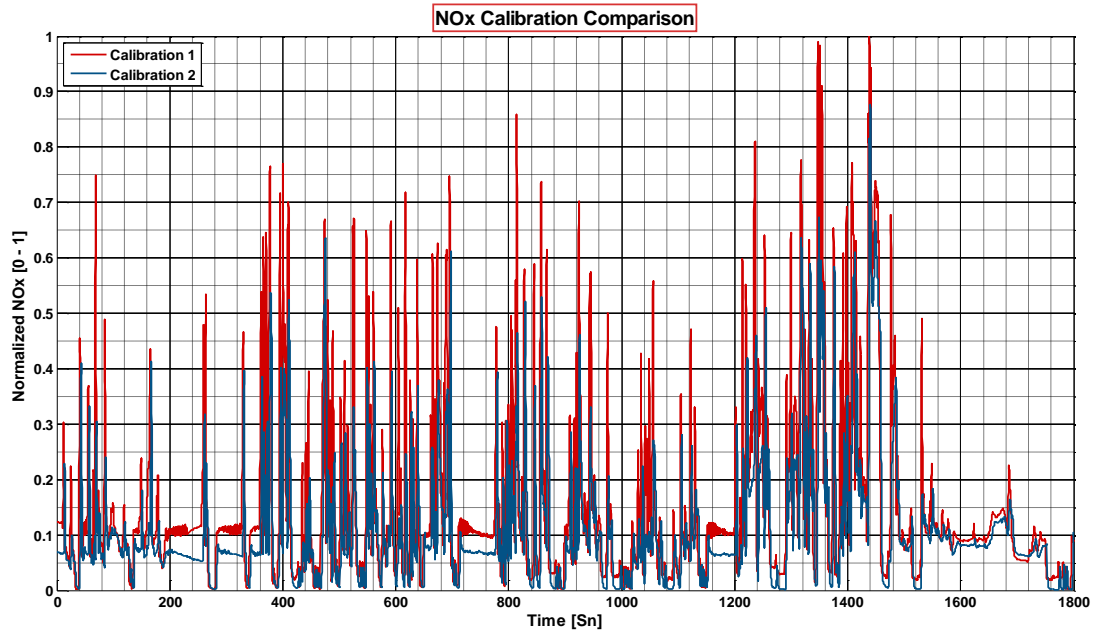


Figure 4.26 : Effetcs of calibration change on NOx values.

In the modeling approach, it is aimed to create an accurate and robust emissions model structure for calibration changes. Furthermore, it is purposed that, the model inputs should be easily feed from a mean value diesel engine model and from the ECU. The generated emission model is validated with the diesel engine model given in the [27]. It is seen that the model is able to work with the mean value engine model. Moreover, the calibration of the ECU is changed and another validation test is run on the dynamometer. The collected data is used in the validation simulation. And it is seen that the generated model structure has capable of tracing the validation data.

5. CONCLUSION

In this work, NO_x formation of a light duty diesel engine is estimated with a high accuracy for steady state and transient engine operating points. The desired accuracy for soot estimation could not be reached. The inputs used in the estimation methods, are chosen according to the empirical experiences and literature survey. The modelling input parameters are engine speed, mass air flow in to the cylinder, manifold absolute pressure, quantities and timings of pilot and main injections, rail pressure and crank angle of combustion center. The two types of methods are applied for estimation. The aim of the thesis is to create a model structure that can be used for diesel engine control algorithm development and diesel engine calibration purposes. Therefore, the generated model shall be used in real time applications like hardware in the loop simulations.

The first method is the symbolic regression based estimation. With this method, 2 different scenarios are applied. In the first scenario, a base map output is multiplied with a set point deviation estimator. The equation structure of the deviation estimator is created by a genetic programming based symbolic regression algorithm. For this purpose, a MATLAB toolbox called GPTIPS has been used. Moreover, during the literature survey in many works, it is seen that the mass burned fraction has a great impact on the formation of NO_x and PM. Therefore, with the scope of 1st scenario, the crank angle information of the combustion center is also used as a virtual sensor. Same positive effects for our modelling approach are tried to be observed. To calculate the mass burned fraction rates, it is seen that mainly 3 types of approaches are available the first one defines the mass burned fraction as the cumulative heat rate divided by the total heat rate. This means that the rate of heat release is proportional to the mass burned fraction. The second method claims that there are 2 types of source for pressure deviation. The first one is the crank rotation. Due to the diesel engine itself is a slider crank mechanism, it is working like a volumetric pump. So the first source of the pressure is the volume change. The second one is the combustion. Because we have the total pressure information

coming from in cylinder pressure sensor. The total pressure change due to the combustion is calculated after subtracting the total pressure change causing from the volume change by using the ideal gas law relations. Another method says that instantaneous change of pressure due to the combustion divided by the total pressure change caused by the combustion gives the crank angle based burned mass fraction rates. By this way, we created the mass burned fraction values. However, these approximation requires the knowledge of instantaneous in cylinder pressure information, this method could not be applied easily in real time applications. Instead a well known wiebe function is used. However, the main problem of the wiebe function is that it requires the information of start of combustion and end of combustion. So, further analysis has been carried on the in cylinder information. Finally, some acceptable assumptions are made regarding to the start of combustion and end of combustion. From the literature survey it is seen that the end of combustion is almost around the 430-435 crank angle degrees. From our in cylinder pressure information 433 -434 crank angles are also observed. However, to be honest, the most challenging information is the start of combustion. Infact we have the information of pilot and main injection informations coming from the ECU, estimation of the ignition delay is not an easy task. Constraints, coming from the real time and faster than real time capability, it is assumed that the ignition delay is approximately 21 crank angle. The wiebe function showed acceptable trace with the value of mass burned fraction curves derived from the cylinder pressure. After creating the virtual sensor values of combustion center information, it is used in the symbolic regression approaches as the input of the models. Because the start of combustion used in the wiebe function is approximate with start of main injection plus assumed ignition delay. Start of main injection and crank angle of combustion center is not used in the same parameter set. From the results, observed from the symbolic regression approach, I can say that the mass burned fraction information that I calculated is not a challenging information near the start of main injection. I observed almost same closer effects on the NO_x and PM formation. The second scenario of the symbolic regression approach is removing the base map from the model structure. A significant result also could not be observed. I can say that, symbolic regression approximation is not a valid method for engine out emissions estimation because of its high nonlinearity. Moreover, results taken from the symbolic regression is not reproducible.

The final method that gives acceptable results on the NO_x , and better results than the symbolic regression is the polynomial based regression approach. With this approach, I calculated the NO_x values vary fast with acceptable error rates for steady state and transient testings. The model has 3 parts, approximates the delays coming from mass transformation and sensor delays during the transient testing. The second part simulates idle operating mode emissions and the last part simulates the non idle operating range of the diesel engine.

As a consequence, the main goal of the thesis was to create an engine emissions model that shall be use the output of a mean value diesel engine model as input parameters. This goal has been achieved with respect to NO_x . On the other hand, as a target of this work, we intend to create a model that could work faster than real time, this also overcome. Another goal was, the model should be capable of steady state and transients even if a calibration occurs. This could not be experienced because, we do not have a such data. But while collecting data, because the setpoints are swept, the accuracy of the model can be acceptable and it can follow the same trace with validation data. As a future work, soot model can be estimated with a phenomenological methods like Hiroyasu method. But I can say that the it is not an easy task to estimate the particulate matter with empirical methods.

REFERENCES

- [1] **Michael Benz, Christopher H. Onder and Lino Guzzella**, (2010), Engine Emission Modeling Using a Mixed Physics and Regression Approach, Journal of Engineering for Gas Turbines and Power, ETH Zurich, Switzerland, APRIL.
- [2] **Johann C. Wurzenberger, Sophie Bardubitzki and Peter Bartsch**, (2011), Real Time Capable Pollutant Formation and Exhaust Aftertreatment Modeling-HSDI Diesel Engine Simulation, SAE, University of Ljubljana, Slovenia, DECEMBER.
- [3] **Qingyun Su**. (2009), Detailed Modeling and Simulation of Automotive Exhaust NOx Reduction over Rhodium under Transient Lean-Rich Conditions Unpublished doctoral dissertation, University of Heidelberg, Heidelberg, Germany, June.
- [4] **Lino Guzzella**, (2009), Introduction to Modeling and Control of Internal Combustion Engine Systems, ETH Zurich, Zurich, Switzerland, September.
- [5] **Urs Christen, Katie J. Vantine and Nick Collings**, (2001), Event-Based Mean-Value Modeling of DI Diesel Engines for Controller Design, SAE , University of Cambridge, Michigan, USA, March.
- [6] **Josef S., Daniel A., Klaus S. Oppenauer , Luigi del Re** (2011), Gray Box Diesel Engine Soot Emission Modeling Based on Two-Color Spectroscopy Measurements, SAE, Kepler University, Linz, September.
- [7] **Hiroyasu, H.**, (1985), Diesel Engine Combustion and Its Modeling, Proceedings of COMODIA Symposium on Diagnostics and Modeling of Combustion in Reciprocating Engines, Tokyo, Japan, pp. 53–75.
- [8] **Xiuyong S., Xinqi Q., Yuanyuan Z.**, (2009), Study on the Mechanism of Soot Formation and Oxidization in a DI Diesel Engine Using Postinjection, Energy & Fuels, Shandong Jiaotong University, Shandong, China, March
- [9] **Jonas A., Oscar C., Lino G. ,** (2012) A fast and accurate physics-based model for the NOx emissions of Diesel engines, ScienceDirect, ETH Zurich, Zurich, Switzerland, September.

- [10] **Stan L-C, Mitu D. ,Elena** , (2010) , Simplified mechanism used to estimate the NO_x emission of diesel engine, In: Proceedings of the 2nd international conference on manufacturing engineering, quality and production systems, Maritime University, Constanta, Romania.
- [11] **Arregle J, Lopez JJ, Guardiola C, Monin C.**, (2010), Sensitivity study of a NO_x estimation model for on-board applications, SAE, Universidad Polit cnica de Valencia, Detroit, USA, April.
- [12] **Arregle J, Lopez JJ, Guardiola C, Monin C.**, On board NO_x prediction in diesel engines: a physical approach. In: Automotive model predictive control, Springer London, Berlin,Germany.
- [13] **T. L. Chan , X. B. Cheng** , (2007), Numerical Modeling and Experimental Study of Combustion and Soot Formation in a Direct Injection Diesel Engine, Energy & Fuels, Wuhan, Huazhong UniVersity of Science & Technology, China, February.
- [14] **Amsden, A., Ramshaw, J., O'Rourke, P., and Dukowicz, J.**, (1985), Kiva: A Computer Program for Two- and Three-Dimensional Fluid Flows With Chemical Reactions and Fuel Sprays, Los Alamos National Laboratory, Technical Report No. LA-10245-MS.
- [15] **R. Tatschl, P. Priesching, J. Ruetz, Th. Kammerdiener**, (2007) , DoE Based CFD Analysis of Diesel Combustion and Pollutant Formation, SAE, AVL List Gm bH, Austria.
- [16] **Hu Wang , Rolf D. Reitz , Mingfa Yao**, (2012) , Comparison of Diesel Combustion CFD Models and Evaluation of the Effects of Model Constants, SAE, Tianjin Univ, Wisconsin, USA.
- [17] **Philipp A. , Oliver L. , Reiner S. and Volker W.** , (2002) , CFD Simulation of Diesel Injection and Combustion, SAE ,FEV Motorentechnik GmbH, Aachen, Germany, March.
- [18] **Michael Benz, Christopher H. Onder and Lino Guzzella**, (2010), Engine Emission Modeling Using a Mixed Physics and Regression Approach, Journal of Engineering for Gas Turbines and Power, ETH Zurich, Switzerland, APRIL.
- [19] **Eriksson, L. and Andersson**, (2002), An Analytic Model for Cylinder Pressure in a Four Stroke SI Engine, 'SAE', Link ping University, Sweden, March.
- [20] **Jason Meyer** , (2007), Engine Modeling of an Internal Combustion Engine With Twin Independent Cam Phasing, Thesis, Ohio State University,USA.

- [21] **Ahmed Soliman , Feilong Liu**, (2012), An Experimental Study on Engine Dynamics Model Based In-Cylinder Pressure Estimation, SAE, University of Cambridge, UK January.
- [22] **Michael Benz**, (2010), MODEL-BASED OPTIMAL EMISSION CONTROL OF DIESEL ENGINES, Doctoral Dissertation, ETH ZURICH, Switzerland.
- [23] **Url-1** < <https://sites.google.com/site/gptips4matlab/>>, date retrieved 17.12.2012.
- [24] **John Koza**, (1992), Genetic Programming: on the programming of computers by means of natural selection,
- [25] **Krzysztof Z. Mendera, Andrzej Spyra, Michał Smereka**, (2002), MASS FRACTION BURNED ANALYSIS, Journal of KONES Internal Combustion Engines, Institute of Internal Combustion Engines and Control Engineering.
- [26] **Patrick F. Flynn**, (1999) , Diesel Combustion: An Integrated View Combining Laser Diagnostics, Chemical Kinetics, and Empirical Validation, Society of Automotive Engineers International Congress and Exposition, Detroit, March.
- [27] **Unver Bulent**, (2013) , Dizel Motorların Modellenmesi, Modele Dayalı Hava Yolu Ve Emisyon Kontrolörü Geliştirilmesi / Uygulanması, Ph.D. Thesis, Istanbul Technical University, Istanbul, Turkey.
- [28] **AVL**, (2005) , Smoke value measurement with the filter-paper-method, Application Notes, Graz, Austria, June.
- [29] **Sasaki H., David S.**, (2010), Development of an Al₂O₃/ZrO₂-Composite High-Accuracy NO_x Sensor, 'SAE', NGK Spark Plug Co Ltd., USA, April.

CURRICULUM VITAE



Name Surname: Yiğit Koyuncuoğlu
Place and Date of Birth: İzmir 24.04.1987
Address: Dr. Fahri Atabey Cad No :118 Daire 4 Üsküdar/
İstanbul
E-Mail: yigit_koyuncuoglu@hotmail.com
B.Sc.: İzmir Yüksek Teknoloji Enstitüsü

Professional Experience and Rewards:

ITU - Mechatronics Research Center : Research Engineer 09.2010-02.2011

Ford-Otosan - Product Development Engineer 02.2011-.....

List of Publications and Patents:

Apak, A. ; Koyuncuoğlu, Y. ; Heceoglu, H. ; Samur, A.B. ; Dogan, U. ; Kurtulus, E. ; Unver, B. ; Gokasan, M. ; Mugan, A.; (2011); Construction of an Electrical Minibus; IEEE;Mechatron. Center, Istanbul Tech. Univ., Istanbul, Turkey